

Fiber Reinforced Solids Possessing Great Fracture Toughness: The Role of Interfacial Strength

Final Technical Report

NASA Grant
NGR 23-005-528

August 1, 1972 - July 31, 1974

NASA Technical Officer
W. B. Fichter
Materials Division
Fracture Mechanics Section
Langley Research Center
Hampton, Virginia 23665

Principal Investigator
A. G. Atkins
The University of Michigan
Department of Mechanical Engineering
2046 East Engineering Bldg.
Ann Arbor, Michigan 48104

Reproduced by
NATIONAL TECHNICAL
INFORMATION SERVICE
U.S. Department of Commerce
Springfield, VA. 22151



(NASA-CR-138946) FIBER REINFORCED SOLIDS
POSSESSING GREAT FRACTURE TOUGHNESS: THE
ROLE OF INTERFACIAL STRENGTH Final
Technical Report, 1 Aug. 1972 - 31 Jul.
(Michigan Univ.) -74 p HC \$6.75 CSCL 20K
75

G3/32
Unclas
54128

N74-29311

PRICES SUBJECT TO CHANGE

N O T I C E

THIS DOCUMENT HAS BEEN REPRODUCED FROM THE BEST COPY FURNISHED US BY THE SPONSORING AGENCY. ALTHOUGH IT IS RECOGNIZED THAT CERTAIN PORTIONS ARE ILLEGIBLE, IT IS BEING RELEASED IN THE INTEREST OF MAKING AVAILABLE AS MUCH INFORMATION AS POSSIBLE.

Final Technical Report


Fiber Reinforced Solids Possessing
Great Fracture Toughness: The
Role of Interfacial Strength

NASA Grant
NGR 23-005-528

August 1, 1972-July 31, 1974

NASA Technical Officer
W.B. Fichter
Materials Division
Fracture Mechanics Section
Langley, Research Center
Hampton, Va. 23665

Principal Investigator
A. G. Atkins
University of Michigan
Dept. of Mechanical Engineering
2046 East Engineering Bldg.
Ann Arbor, Mi. 48104



NGR 23-005-528

This Final Technical Report

Supersedes all previous communications

(such as those of Nov. 1972, April 1973, Nov. 1973 and April 1974)

in regard to descriptions,

results, mathematical analyses, etc.

No other report in NTIS System

N-a

INTERMITTENT BONDING
FOR
HIGH TOUGHNESS/HIGH STRENGTH
COMPOSITES

BY

A. G. ATKINS

Department of Mechanical Engineering
University of Michigan
2046 East Engineering Building
Ann Arbor, Michigan

v-b

Contents

Summary	i
List of Symbols & Abbreviations	ii,iii
Data Sheet	iv
1. Introduction	1
2. Mathematical Model	5
3. Testpieces & Experimental Results	9
4. Discussion	15
5. Conclusions	23
References	25
Appendix A	26
Appendix B	33
Appendix C	34
Captions for Figures	43
Figures	45 et seq.

N-C

SUMMARY

High strength and high toughness are usually mutually exclusive in brittle filament/brittle matrix composites. The high tensile strength characteristic of strong interfacial filament/matrix bonding can, however, be combined with the high fracture toughness of weak interfacial bonding, when the filaments are arranged to have alternate sections of high and low shear stress (and low and high toughness). Such weak and strong areas can be achieved by appropriate intermittent coating of the fibers. Boron-epoxy composites of volume fraction 0.2-0.25, have been made in this way which have fracture toughnesses of over 200 kJ/m^2 , whilst retaining rule of mixtures tensile strengths ($\sim 650 \text{ MN/m}^2$). At the volume fractions used, this represents K_{IC} values greater than $100 \text{ MN/m}^{3/2}$.

An analysis is presented for toughness and strength which demonstrates, in broad terms, the effects of varying the coating parameters of concern. Results show that the "toughness" of interfaces is an important parameter, differences in which may not be shown up in terms of interfacial "strength."

Some observations are made upon methods of measuring the components of toughness in composites.

List of Symbols and Abbreviations

A_{nom}	Nominal cross sectional area of test-specimen in path of crack
C	Coating fraction (decimal l_c/l_r).
D	Average distance of fractured filament from plane of gross fracture.
d	filament diameter
E	Young's modulus
H	Height of edge crack testpiece arms
h	Pulled-out relative slip distance
K	Stress intensity factor
L	Finite size of testpiece or length of discontinuous filament
l	Length
N	Number of filaments
n	Ratio of finite length of filament to repeat length ($=L/l_r$)
PUV	Polyurethane varnish
R	Fracture toughness
RoM	'Rule of mixtures'
SVG	Silicon vacuum grease
T	Ratio of coated to uncoated interfacial shear strengths
v	Volume fraction
λ	Ratio of repeat length to filament diameter
ρ	Ratio of coated toughness to uncoated toughness
σ	Tensile stress
τ	Shear Stress
ψ	Ratio of uncoated critical length to repeat length, $(l_{crit})_{uc}/l_r$.

Superscripts

τ' Interfacial shear stress during pull-out

Subscripts

I,II Fracture toughness crack opening modes

av Average

c Coated

crit Critical

f Filament

if Interface

m Matrix

r Repeat length

uc Uncoated

DATA SHEET

Filaments:

$$\sigma_f = 3.45 \text{ GN/m}^2$$

$$E_f = 380 \text{ GN/m}^2$$

$$d = 140 \text{ }\mu\text{m}$$

Matrix:

$$\sigma_m = 81 \text{ MN/m}^2$$

$$E_m = 2.48 \text{ GN/m}^2$$

$$R_m \approx 2-3 \text{ kJ/m}^2$$

$$\tau_m \approx 69 \text{ MN/m}^2$$

Composites:

$$(l_{crit})_{uc} = \frac{\sigma_f d}{2\tau} \rightarrow 3.5 \text{ mm}$$

$$\psi = \frac{(l_{crit})_{uc}}{l_r} \rightarrow \begin{cases} 0.18 & \text{for } l_r = 19 \text{ mm} \\ 0.14 & \text{for } l_r = 25 \text{ mm} \\ 0.07 & \text{for } l_r = 51 \text{ mm} \end{cases}$$

$$\lambda = \frac{l_r}{d} \rightarrow \begin{cases} 136 & \text{for } l_r = 19 \text{ mm} \\ 181 & \text{for } l_r = 25 \text{ mm} \\ 363 & \text{for } l_r = 51 \text{ mm} \end{cases}$$

$$\text{for } C = 0 \quad \sigma_c = 650-700 \text{ MN/m}^2$$

$$\text{for } C = 1 \quad \sigma_c = \begin{cases} 500 \text{ MN/m}^2 & (\text{SVGT}) \\ 450 \text{ MN/m}^2 & (\text{PUV}) \end{cases}$$

1. Introduction

Fracture in brittle matrix/brittle filament composites where the interfacial bond between fiber and matrix is strong often results in a fast matrix crack perpendicular to the filaments. Usually such an energetic crack breaks through all filaments in the path of the crack and complete fracture ensues. Even though shear debonding, of average length $l_{crit}/4$, may occur during fracture since the filaments will not necessarily break in the plane of a matrix crack, the associated "surfaces" contribution to toughness will be relatively limited because l_{crit} is itself small [1].* Similarly, the contribution to toughness from Piggott/Fitz-Randolph stress redistribution [2,3] is limited by the critical length, as is that from Cottrell/Kelly pull-out [4].

A general increase of l_{crit} by lowering the filament/matrix shear bond will increase toughness, as discussed by Marston et al [1]. In that paper, it was shown that a relationship between strength (σ) and total composite toughness (R) could be developed by recognizing that in general terms $R \propto 1/\tau$ where τ is the shear strength of the interfacial bond. In the case of the boron/epoxy system for which data were presented in [1], the surface condition of the as-received B/W filaments was such that when made up into composites with EPON-828 epoxy, strengths in the region of the rule of mixtures (RoM) value were attained. When the surface condition was altered by continuously coating the filaments with

* Numbers in square brackets are references contained at the end of the report.

various substances, the strengths fell off and the toughness decreased (with strong interfaces), or increased (with weak interfaces). In the latter case, if the interfaces were sufficiently weak, there could be the possibility of introducing an additional contribution to toughness, viz: Cook/Gordon tensile debonding ahead of the crack [5]. Such a mechanism, which is usually absent in conventional strongly bonded composites, may blunt and slow down cracks or arrest them completely.

However, weak interfaces throughout the composite can reduce the tensile strength quite significantly. Depending on the circumstances, perhaps 1MN/m^2 in tensile strength is "lost" for every 1kJ/m^2 "added" to toughness in laboratory testpieces; this follows from equation (16) of reference [1] applied to boron/epoxy. The question that presents itself is whether there are any means by which the RoM tensile strength can be maintained along with high toughness values.

Marston [6] suggested that providing there were "enough" regions of high interfacial shear stress to ensure that the rule of mixtures strength was picked up, the rest of the composite could have quite weak interfacial bonds. Were such a composite to be laid up randomly with respect to weak and strong regions, both high strength and high toughness should be produced simultaneously. For if the lengths of the strongly bonded regions are greater than the critical length associated with that strong interfacial τ , the filament strength would be attained, whilst at the same time, those weak interfaces situated randomly ahead of any running cracks would serve to blunt the cracks by debonding.

The concept is shown schematically in Figure 1. Weakly and strongly bonded interfaces can be achieved by intermittently coating the filaments with some suitable substance before composite lay up.

How interfacial properties other than shear strength are affected by the coating procedure is an interesting and vital question, because it is probably the "toughness" of the interface that is of ultimate concern rather than the "strength". The tensile debonding envisaged by Cook and Gordon is fracture in mode I of fracture mechanics nomenclature*; the shear debonding implicit in the Outwater/Murphy analysis for toughness is fracture in the "forward sliding" mode II. The difference in modes was not clearly brought out in reference [1]. Each mode has its own toughness, R_I and R_{II} , the explicit relationships of which to interfacial tensile and shear strengths are not obvious. Results for silicon vacuum grease (SVG) and polyurethane varnish (PUV) coatings are reported later in this paper. The uncoated regions have high interfacial shear stress and the coated regions are "weak", (being reflected in the relative transfer lengths). However, the SVG increased the toughness only modestly, whereas the PUV increases the toughness markedly; respectable tensile strengths were maintained with both coating materials. This emphasizes that the coating material is crucial, and revolves around the ill-understood interfacial toughness properties of the coatings.

* The Roman mode types are used here in the fracture mechanics Volterra dislocation sense, not in the nomenclature suggested by Mullin et al [7], for different types of fracture observed in boron/epoxy systems.

An analysis for the strength and toughness of intermittently bonded brittle filament/brittle matrix composites is presented in the next section. The experimental results show quite strikingly that when appropriate coating materials are employed, strong, high toughness composites can be manufactured in the manner suggested.

2. Mathematical Model

The following analysis is a modification of the treatment presented in [1]. Details of the derivations are given in Appendix I. The broad assumptions are that in a randomly laid up, intermittently bonded composite, the coated and uncoated regions of interfacial shear strengths τ_c and τ_{uc} , may be represented by a rule of mixtures average shear strength τ_{av} given by

$$\begin{aligned}\tau_{av} &= (1-C)\tau_{uc} + C\tau_c \\ &= \tau_{uc} \{1 - C(1-T)\} \quad \text{--- 1.}\end{aligned}$$

where $C = l_c/l_r$, i.e. the ratio of coated length to repeat distance (see Figure 2) and $T = \tau_c/\tau_{uc}$.

The 'fictitious' critical length of the intermittently coated filaments is then given by

$$\begin{aligned}(l_{crit})\tau_{av} &= \frac{\sigma_f d}{2\tau_{av}} \\ &= \frac{(l_{crit})_{uc}}{\{1 - C(1-T)\}} = \frac{\psi \lambda d}{\{1 - C(1-T)\}} \quad \text{--- 2.}\end{aligned}$$

where σ_f is the filament tensile strength, and d the filament diameter. The useful non-dimensional parameters are $\psi = (l_{crit})_{uc}/l_r$, $\lambda = l_r/a$.

In the same manner, we postulate the use of an average interfacial mode II toughness, to represent the behavior of adjacent regions of low and high toughness, given by

$$\begin{aligned}(R_{IIif})_{av} &= (1-C)(R_{IIif})_{uc} + C(R_{IIif})_c \\ &= (R_{IIif})_{uc} [1 - C(1-\rho_{II})] \quad \text{--- 3.}\end{aligned}$$

where $(R_{IIif})_{uc}$ and $(R_{IIif})_c$ are the uncoated and coated interfacial toughnesses, and ρ_{II} is the ratio $(R_{IIif})_c/(R_{IIif})_{uc}$.

The foregoing type of toughness average is not used for mode I debonding, since cracking will not take place in the strong regions according to the Cook/Gordon model. The symbol ρ_I for $(R_{Iif})_c / (R_{Iif})_{nc}$ is however used later.

(a) Tensile Strength

For intermittently bonded filaments, the fiber load build-up may take place at low or high interfaces, or indeed over both types of interface, as shown schematically in Figure 3. With the use of τ_{av} to account for the different interfacial shear strengths, we can write for the RoM tensile strength

$$\begin{aligned}\sigma &= (1 - v_f) \sigma_m + v_f \sigma_f \left[1 - \frac{\sigma_f d}{4 \tau_{av} L} \right] \\ &= (1 - v_f) \sigma_m + v_f \sigma_f \left[1 - \frac{\psi}{2n \{1 - C(1 - T)\}} \right] \quad \text{--- 4.}\end{aligned}$$

where v_f is the filament volume fraction, σ_m the matrix tensile strength and L the finite size of the testpiece or length of the filament. The non-dimensional parameter n is given by L/l_r .

For $C = 0$, equation (4) degenerates to the expression for continuously coated filaments [1]. At $C = 1$ (and therefore $T = 1$), the (lower) RoM tensile strength appropriate to the (lower) τ_c is given. Note that at large C , the uncoated length is shorter than its own uncoated critical length, thus reducing its shear transfer potential, and thus contributing to the fall in σ with C . It may be shown from equation (1) that the value of C at which this occurs is given by

$$C > \frac{2 - \psi}{2(1 - T)}$$

at which time more than one repeat distance is required to get the filament stress up to σ_f (Fig.3). The upper bound to σ is the uncoated RoM value itself, when load transfer happens to occur over regions of (large) τ_{uc} , providing that they are as long as their own critical length.

(b) Fracture Toughness

According to reference [1] the total toughness, for continuously coated filaments, is given by

$$R_{total} = R_{surfaces} + R_{redist} + R_{pull-out} \quad (6)$$

where $R_{surfaces}$ relates to debonding (mode I or II or both), R_{redist} relates to Piggott/Fritz-Randolph stress redistribution, and $R_{pull-out}$ relates to Cottrell/Kelly pull-out.

An additional component, $R_{Cook/Gordon}$, must be added to equation (6) if tensile debonding ahead of the running crack takes place. It turns out that the Cook/Gordon mechanism itself is a comparatively small toughness sink; however, the associated additional debond lengths in the presence of Cook/Gordon debonding significantly increase the pull-out lengths and hence the total toughness. Using equations (1) and (2), and other assumptions detailed in Appendix I, we obtain for intermittently bonded composites

$$R_{surfaces} = (1-v_f)R_m + v_f \cdot \psi \cdot \lambda \left\{ \frac{1 - C(1-\rho_I)}{1 - C(1-T)} \right\} (R_{fI})_{uc} \quad (7)$$

$$R_{Cook/Gordon} = 4v_f C^2 \lambda \rho_I (R_{fI})_{uc} \quad (8)$$

($\rho_I \ll 4 \times 10^{-2}$ or 4×10^{-3}).

$$R_{\text{redist}} = \frac{v_f \cdot \sigma_f^2 \psi \lambda d}{3 E_f \{1 - c(1-T)\}} \quad (9)$$

For $R_{\text{pull-out}}$, two pairs of formulae are given—(with or without Cook/Gordon debonding)—depending upon a constant or varying interfacial stress during pull-out. We have

$$R_{\text{pull-out}} = v_f \tau' \psi \lambda h / [1 - c(1-T)] \quad (10)$$

(for constant τ' , no Cook/Gordon), and

$$R_{\text{pull-out}} = v_f \tau' \lambda h \left[\frac{\psi}{[1 - c(1-T)]} + 2c \right] \quad (11)$$

(for constant τ' , with Cook/Gordon), or,

$$R_{\text{pull-out}} = v_f \tau' \psi \lambda h \quad (12)$$

(for τ' varying according to $\tau' [1 - c(1-T)]$, no Cook/Gordon), and

$$R_{\text{pull-out}} = v_f \tau' \lambda h \left[\psi + 2c \{1 - c(1-T)\} \right] \quad (13)$$

(for τ' varying as above, and with Cook/Gordon).

The total fracture toughness is given by the sum of the appropriate equations (7)-(13). This is discussed later, along with some questions that are raised regarding the magnitudes of the different contributions.

Note that equations (7) and (8) seem to indicate paradoxically that the greatest R would come from the largest values of ρ (i.e. increased interfacial coated toughness). The Cook/Gordon expression however only applies when ρ is very small, and in the case of equation (7) the implication of large toughness comes about from the fact that, on average, every filament fracture is accompanied by a debond length of $l_{\text{crit}}/4$ so that if the coated critical lengths are long (because of low τ_c), the tougher the interface the better. But some filament fractures will have zero debond length, and these are the ones that set up energetic matrix cracks which clearly will not be arrested by tough interfaces in their path.

3. Testpieces and Experimental Results

Tensile and toughness specimens were made from layers of intermittently bonded epoxy composite tape manufactured on a drum apparatus with a device for coating the filaments before lay-up (Fig. 4). The tape is similar to Avco proprietary "Rigidite, Prepreg" tape* except that the commercial tape has a filament surface condition that is uniform throughout. Our tape consists of a 250 μm monolayer of B/W filaments in EPON 828 epoxy, backed, for ease of handling, on 760 mm wide nylon scrim cloth of thickness about 50 μm . The tapes are layed up on the periphery of a drum, the volume fraction of filaments being varied by altering the wrapping rate. The coating device is pneumatically operated, and "crimps" the filament with coating material, the coated/uncoated lengths being altered by the frequency of operation. The arrangement clearly does not give a truly random lay-up, but when the repeat distances are not multiples of the drum circumference, alternate coated and uncoated regions are presented to a running crack; additionally test specimens consisted of many layers of tape, again helping the random lay-up concept. Tapes are stored in a refrigerator with the epoxy in the half-cured B-stage, complete curing (12 hours at 120°C followed by oven cooling) taking place after specimens consisting of various layers have been made.

To investigate the intermittent bond analysis, tapes were manufactured for a range of values of ψ , λ and C. The principal coating materials were silicon vacuum grease (as used by

* Avco Systems Division, Lowell, Mass. U.S.A.

Marston [5] in his preliminary experiments) and polyurethane varnish. The repeat distances (l_r) were variously 19 mm, 25.4 mm, and 51 mm which gave $0.05 \sim \psi \sim 0.13$, and $135 \sim \lambda \sim 360$. Independent tensile tests of 100% coated specimens suggested that $T = 0.06$ (silicon vacuum grease) and $T = 0.05$ (polyurethane). The toughness ratios ρ were not known independently, but values can be inferred from the experimental data, as discussed later.

Tensile and toughness specimens were made from the same tape for a given combination of parameters. The tensile specimens consisted of 2 layers of the tape, in 100 mm x 6 mm strips, with end tabs reinforced by additional layers of tape. Marston et al [1] measured composite toughnesses using Tattersall and Tappin 3-point bending "roof" specimens. To make comparison with the earlier data, some 5 mm x 5 mm x 35 mm Tattersall and Tappin specimens were made up from the tapes, but for reasons explained later, most toughness measurements in the present series were made on flat sheet edge-crack specimens, akin to ASTM "compact tension" specimens in profile. These consisted of ten layers of tape in 76 mm x 76 mm panels as shown in Figure 5. Originally it was intended to load the specimens at section AA, but bearing failures occurred at the holes and the crack velocities did not allow easy visual tracking in the less tough test-pieces. Steel outriggers were added to the specimens, which reduced both the crack load and the crack velocity. To prevent the composite arms above the crack from shearing off under load, two outside layers of tape on each side of the specimens were arranged with the filaments parallel to the crack. The central core of the specimen thus consisted of six unidirectional filaments

perpendicular to the starter crack, where, within the limitations of the specimen and tape preparation method, the coated and uncoated layers occurred randomly relative to each filament.

Fracture toughness in the edge crack specimens was measured for increments of crack area, using Gurney's sector area technique [8] shown in Figure 6 (the crack length being monitored during every test and the testing machine load-extension trace "pipped" accordingly). Separate tests showed that the matrix work of fracture in the outside layers of tape did not contribute significantly to the toughness. The load/extension plots showed some curvature before crack propagation especially in the high percentage coated samples. Upon unloading, after some crack propagation, the tougher testpieces showed marked "displacement irreversibility", i.e. the specimens remained "yawed open". Although geometric interference of filaments still bridging the crack obviously contributed to this effect, the question arises as to whether generalized yielding has occurred. Irreversibility at regions remote from the crack faces is a bane of fracture toughness testing of high toughness/low strength solids. If specimens are saw-cut along the crack into virgin material beyond the crack tip "plastic zone" and they subsequently close up, it may be assumed that all irreversible work has been confined to areas contiguous with the crack faces. Then the whole area under the load/extension plot may be attributed to work of fracture. Most of our specimens did close up. However, in the highest percentage PUV coated specimens, it was difficult to propagate cracks at all, and buckling delamination at the back face of the testpiece, or shear deformation along planes perpendicular to the crack in the specimen "arms", termin-

ated the experiments (Figure 7). Hence the toughness values at the highest percentage coatings in PUV edge-crack specimens are not known with confidence, but the quoted values if anything are perhaps low (see Appendix C).

The toughness data from the Tattersall and Tappin PUV testpieces did not show these effects. They did, however, display a curious behavior, with the toughness values levelling off after about $C = 0.5$, rather than carrying on rising at large C . These effects are discussed later.

Tensile and edge-crack fracture toughness results for both silicon vacuum grease and polyurethane coatings are plotted against C in Figures 8 and 9. The tensile data remains at or about the RoM value until C gets greater than 0.8. The fall in σ at very large C is anticipated from the analysis in section 3.

The toughness results with silicon vacuum grease coating fall slightly with increase of C , but beyond $C = 0.4$, R becomes modestly greater than the "completely uncoated" (i.e. $C = 0$) case. The edge crack and Tattersall and Tappin data all essentially agree: for $V_f = 0.25$, and $C = 0$, $R = 45-50 \text{ kJm}^2$; for $C = 1.0$, $R = 60-65 \text{ kJ/m}^2$.

In contrast, the polyurethane coatings gave marked improvements in toughness for increased percentage coating. In the edge-crack specimens, with $V_f = 0.25$, toughnesses about 100 kJ/m^2 are produced for $C = 0.5$, and values around $250-300 \text{ kJ/m}^2$ occur at large C . As previously mentioned, these latter toughness values may not be precise. The Tattersall and Tappin data levelled out at some 110 kJ/m^2 for all $C > 0.5$, which suggests that one or more components of the toughness in the

* The results are different from reference [1], since larger diameter, stronger, boron filaments have recently been employed, viz: 140 instead of $100 \mu\text{m}$ diameter, 3.45 in place of 2.96 GN/m^2 for σ_f ; V_f is also different.

edge-crack specimens at large C, failed to contribute to cracking in the 3-point beam bending situation.

To have some feel for the interfacial shear stresses active during pull-out, some of the 'used' edge-crack specimens that were partially cracked through were regripped above the original uncracked portion and pulled in tension. After the crack had propagated across the relatively narrow section, and the crack faces had separated, the work subsequently performed in pulling the fibers out was measured from the testing machine chart. Some of the fibres had already been broken in the original edge-crack tests, and the remainder were broken when the crack faces were separated in these pull-out measurements. Inspection of the pull-out lengths enabled estimates for τ' to be obtained from the expression for work in pulling out one filament over length h , viz: $\frac{1}{2}\tau'\pi dh^2$. The PUV pull-out lengths were quite long, which helped experimentation.

During pull-out, the interfacial frictional stress for the uncoated samples was about 10 MN/m^2 , which should be contrasted with the matrix shear stress of some 70 MN/m^2 . For most of the PUV coated samples, however, the interfacial shear stress during pull-out seemed to be independent of C, having the approximate value of 2 MN/m^2 . This is perhaps surprising, as one might have expected a frictional stress decreasing with increasing C. The SVG data were rather inaccurate, since the pull-out lengths were considerably shorter. Later in this paper, we will see that to obtain agreement between theory and experiment for the toughness data, we would like to have τ' constant for PUV, but varying for SVG.

Finally, to see "how tough" a testpiece could be made, some $V_f = 0.5$ C = 0.8 tapes were manufactured and layed up into a 12 layer 4 mm thick edge-crack specimen, with 8 layers perpendicular to the crack line and 4 layers parallel to the crack. Instead of crack-ing, the testpiece "yielded" in the arms, giving the warped shape shown in Figure 10 on unloading. No estimate for fracture toughness is thus available (see Appendix C). We can find a bound on it, however, in the following way: Gurney & Hunt [8] and Hahn et al [9] have shown that generalized yielding in the testpiece, rather than crack propagation, should be expected when

$$H < \frac{(1.5 \sim 3.0) ER}{\sigma_y^2}$$

where H is the height of the testpiece "arms", and σ_y the yield strength. Using the following values with $V_f = 0.5$, viz: $E = (0.5)(380) \text{ GN/m}^2$, $\sigma_y = (0.5)(3.45) \text{ GN/m}^2$, and inserting $H = 38 \text{ mm}$, we have

$$R > (200 - 400) \text{ kJ/m}^2$$

For reference, uncoated specimens with $V_f = 0.5$ (such as test-pieces made up from as-received Avco Prepreg tape) give $R \sim 100 - 120 \text{ kJ/m}^2$.

4. Discussion

The tensile strengths of $0.2 V_f$ composites with filaments fully coated with silicon vacuum grease and polyurethane varnish were about 500 MN/m^2 and 450 MN/m^2 respectively. The 'as-received' strength with no coating was some $(650-700) \text{ MN/m}^2$. For the size of tensile testpieces used, $\Psi/n \approx 0.03-0.05$. Applying equation (4) to the fully coated samples, with $\sigma_f = 3.45 \text{ GN/m}^2$, $\sigma_m = 81 \text{ MN/m}^2$ and $d = 140 \mu\text{m}$, it would appear that T was about 0.06 for SVG and about 0.05 for PUV. Using these values, equation (4) has been plotted out versus C on Figure 8. The general agreement with experimental tensile results at various percentage coatings is reasonable.

The longest pull-out lengths that were observed after completion of the experiments to measure τ' (the interfacial shear stress during pull-out) agreed reasonably well with $(l_{crit})_{rav}/2$ given by equation (2) for SVG using $T = 0.06$. In the case of PUV, the longest pull-out lengths were consistently greater than $(l_{crit})_{rav}/2$ with $T = 0.05$. If Cook/Gordon debonding were taking place in the intermittently bonded composites, we should expect the pull-out lengths to be longer. At $C = 0.25$, $(l_{crit})_{rav}/2 \approx 2 \text{ mm}$; with a 25 mm repeat distance, the Cook/Gordon debond length is some 6 mm so that the longest pull-out length may be expected to be about 8 mm. This was what we observed, and at the largest percentage coatings, many filaments pulled out the complete 'half height' of the specimen (Figure 11), since the pull-out lengths (incorporating Cook/Gordon debonding) should be greater than 38 mm. Although general agreement for the longest pull-out lengths was obtained, the average pull-out lengths seemed smaller than $(l_{crit})_{rav}/4$ for SVG and smaller than $[(l_{crit})_{rav}/4] + [Cbr/2]$ for PUV. Nevertheless, the trend of

pull-out lengths seemed to indicate that Cook/Gordon debonding was taking place with PUV coatings, but that it was absent with SVG. The marked difference in toughness values, (although T was not very different between SVG and PUV), confirms this contention.

Comparison with equations (7) thru (13) for the composite toughness is not easy to make without some handwaving about the interfacial toughness values. The matrix toughness itself, R_m , may be independently determined from edge-crack or Tattersall and Tappin testpieces: for the epoxy cure cycle that was employed, R_m (2.5~3.0) kJ/m². The presence of the nylon scrim cloth, in thin edge-crack specimens* made up from tapes containing no filaments, had an insignificant effect. In principle, interfacial toughness in Mode II can be measured by pulling on embedded filaments, but in practice the experiments are difficult to perform (the pull-out experiments described earlier for τ' are, of course, different in nature). Interfacial toughness in mode I does not seem easy to measure. It was argued in reference [1] that substitution of the matrix toughness for the interfacial toughness was a reasonable approximation in continuously coated composites, because if R_{if} (R_{ifuc} in the intermittent bond context) were greater than R_m , matrix material would adhere to the filaments and this was not observed experimentally. A similar postulate is used for intermittently bonded composites where, in addition, the following is suggested for P_{II} : let us assume that the interfacial shear stress is proportional to the mode II stress intensity factor.

* This result is comparable with other results for R_m obtained in thick sections. It is believed, therefore, that the high values for total toughness at large C do not arise from 'thin-plate' plane stress considerations.

Then the ratio of coated and uncoated shear stresses (T) becomes

$$T \approx \frac{(K_{II})_c}{(K_{II})_{uc}} \approx \sqrt{\frac{(R_{ifII})_c}{(R_{ifII})_{uc}}} \approx \sqrt{\rho_{II}}$$

For $T=0.06$, $\rho_{II} \rightarrow 36 \times 10^{-4}$ (SVG); for $T=0.05$, $\rho_{II} \rightarrow 25 \times 10^{-4}$ (PUV).

Equation (7) is not sensitive to such small values of ρ_{II} over the applicable range of variables, so that it is adequate to consider $\rho_{II}=0$ in the toughness expressions, or cancel out the $[1-C(1-\rho_{II})]$ term with the $[1-C(1-T)]$ term (see later.)

With that assumption, and with the values of τ' obtained from the pull-out experiments for SVG and PUV, equations (7)–(13) may be plotted and compared with the toughness data. In general terms, it is readily shown that the equations, which incorporate Cook/Gordon debonding, overestimate the observed SVG results, but are in reasonable agreement with the PUV data. There are, however, some questions regarding the precise algebraic formulations of some of the components of the total toughness.

The form of the pull-out contribution relates back to the behavior of τ' in the pull-out experiments. In the case of PUV, a constant τ' of some 2 MN/m^2 seems to be required to describe the toughness results, whereas for SVG a τ' which diminishes with increasing C is required. Such differences in τ' behavior were broadly observed in the pull-out tests, but the reasons are unclear. Perhaps the interfacial friction stress of the Cook/Gordon debond lengths "biases" the average τ' down to an approximately constant value.

The magnitude of the Piggott/Fitz-Randolph contribution could be one-half of the usually quoted expression, for the following reason. The energy dissipating mechanism is irreversible relative slip between filament and matrix in the presence of 'full' interfacial bonding. In reference [2], the situation was modelled

where the matrix fracture strain was less than the filament fracture strain, so that filaments were stretched relative to the matrix interface before they fractured (a matrix crack perpendicular to a filament having passed ahead of the filament). Irreversible work is thus performed, and when the filament 'sprang back' after fracture, more work was dissipated at the interface. The distance over which slip occurs was shown to be $(l_{crit})/2$ [2]; the 'forward slip' and 'backslip' contributions to toughness were the same, and equal to $\frac{1}{2} \sigma_f^2 (l_{crit}) / 6 E_f$, i.e. one-half of equation (9) as previously quoted. If the filament fracture strain is less than the matrix fracture strain, as is the case for boron/epoxy, presumably the 'forward slip' contribution is absent. The curves superimposed on Figure 9 show both possibilities; the data favour irreversible slip only in one direction.

Thirdly, there is also a question about the magnitude of the Cook/Gordon contribution to toughness. Equation (8) gives values differing by a factor of ten, depending on the magnitude of ρ_I , which in turn depends upon the choice of 1/5 or 1/50 for the critical tensile strength ratio. However, the Cook/Gordon component to total toughness itself is comparatively small, so that it is not possible, from the experimental results, to establish which value of ρ_I is appropriate.

It is instructive to present the magnitudes of the relative contributions to R from the various mechanisms, taking into account the foregoing questions. For PUV, with $R_m \approx 2.6 \text{ kJ/m}^2 \approx (R_{Iif})_{uc}$, $T \approx 0.045$, $\psi = 0.14$, $\lambda = 181$, $d = 140 \mu\text{m}$, $\tau' = 2 \text{ MN/m}^2$ and measuring all toughness values at a crack opening of $h = 0.5 \text{ mm}$ and cancelling $[1 - C(1 - \rho_I)] \approx [1 - C(1 - T)]$, we have from equations (7, 8, 9, and 11

for $V_f = 0.25$,

$$R = 2 + 16 + \frac{6.3(0.7 \text{ or } 1.4)}{[1 - 0.955C]} + (1.9 \text{ or } 19)C^2 + 45 \left[\frac{0.14}{(1 - 0.955C)} + 2C \right]$$

where R is in kJ/m^2 . We see that the contribution from matrix fracture surfaces remains constant at 2kJ/m^2 ; the surfaces contribution from filament debonding also remains constant at about 16kJ/m^2 , (after the cancelling assumption),—the increase in debond area with C being counteracted by a reduction in average $(R_{II \text{ if}})_C$. Piggott/Fitz-Randolph stress redistribution increases with C , the longer l_{crit} of higher C giving longer relative slip distances. The Cook/Gordon contribution increases as C^2 , (i.e. $1.9C^2$ or $19C^2$) but in total terms is a small contributor to composite toughness. However, the increased debond lengths that accompany the Cook/Gordon mechanism produce a significant effect on the pull-out contribution, and the latter is an important part of the total toughness.

At $C=1$, we have

$$\begin{aligned} R &= 2 + 16 + (100 \text{ or } 200) + (2 \text{ or } 19) + 141 + 90 \\ &= 351 \text{ or } 468 \end{aligned}$$

taking the lower and higher values of the debatable terms. On Figure 9 have been superimposed two curves given by the foregoing treatment with high and low values as in the example for $C=1$.

It seems that the results favour the lower curve*; we note, however, that the experimental R values for large C are questionable, and may be low.

* If the existence of Cook/Gordon debonding is doubted, it might be asked whether equations (7, 9, and 10)—with no Cook/Gordon debonding but with the full equation (9) for the Piggott/Fitz-Randolph contribution,—could satisfy the data. Such an analysis fails to agree with the experiments.

For SVG, with $T=0.06$, $\tau'=3 \text{ MN/m}^2$ (varying) and the previous values for the other parameters in equations (7,9, and 12), we have

$$R=2+16+\frac{4.5}{(1-0.94C)}+10$$

where half the Piggott/Fitz-Randolph expression is used. The resulting curve for R vs. C is superimposed on Figure 9.

The Tattersall and Tappin toughness results are interesting. In some ways, this testpiece design is not completely satisfactory since there is a transition from plane stress behavior at the apex of the triangle to plane strain at the base, so that the area under the load/extension curve indicates some ill-defined average toughness. Also, if the triangular section is made by cutting, damaged filaments near the apex also give easy crack initiation. Moreover, the testpiece is strictly unstable, (as may be demonstrated by application of Gurney's crack stability criteria[e.g.11] to experimental compliance data), — although with composites those broken filaments bridging the crack faces, after passage of the crack, do introduce a measure of stability through the pull-out contribution to toughness. ^(see Appendix C') In the present series of experiments with very tough composites, another effect in such small 3-point bending situations came to light.

In the case of SVG, the data essentially agree with the edge-crack results, except that the $C=1$ results are low. For PUV, however, the results are in reasonable agreement with the edge-crack results only up to $C=0.5$; after that, the Tattersall & Tappin data level out at some 110 kJ/m^2 , as opposed to the edge-crack results which continue to increase significantly. It seems as if the pull-out contribution was being limited in some way. Very tough composites have large crack opening displacements before and during

crack propagation; some of our beam specimens 'bottomed-out' (Fig. 12) in our 3-point bending rig before cracking through, for example. This means that the long pull-out lengths which bridge the crack faces in such circumstances are bent to severe "exposed" radii. Engineers' bending theory suggests that the top fibres in one of our Tattersall and Tappin testpieces, bent to a 5 mm radius, suffer a stress of some 5 GN/m^2 . This is greater than the tensile fracture strength of the boron-on-tungsten filaments (circa 3.5 GN/m^2). It would appear that in very tough composites a proportion of fibers break by bending in small beam specimens, thus preventing a full pull-out contribution to toughness. Certainly the pull-out lengths of high C beam specimens seemed short in comparison with those of equivalent tensile or edge-crack specimens. Also, 'double filament fractures' have been observed in the high C PUV beam specimens, i.e. where filaments break inside the beam initially, but also break subsequently across the crack faces. Such short filaments may be removed with tweezers after completion of a Tattersall & Tappin test.

It has been pointed out earlier that filaments, which bridge the crack faces for some time after passage of the crack front, stabilize cracking. If some of the pull-out contribution to toughness is lost at large beam deflections by those filaments fracturing in bending, the load/deflection R locus plots should revert to the natural shape of unstabilized cracks. Figure 13 shows that the shape of the Tattersall and Tappin load/deflection plots at large displacements in high C PUV specimens are different from the corresponding shape at low C, (see Appendix C for additional explanation).

Since the diameters of typical graphite filaments are much smaller than boron-on-tungsten filaments ($\sim 8 \mu\text{m}$ vs. $140 \mu\text{m}$), the bending stresses induced at large deflections in Tattersall & Tappin testpieces made of carbon-polyester composites would be much smaller than the filament fracture stress, so that valid toughness data would seem to be obtainable.

The foregoing observations emphasise the care with which the pull-out contribution to toughness must be treated. Although rarely acknowledged in such terms, "strict" fracture mechanics toughness implies displacement reversibility, i.e. crack testpieces return to the origin of load/displacement plots upon unloading. Pull-out is a frictional contribution to toughness, and unloading the specimen involves additional irreversible work in pushing back "down the holes" those filaments that bridge the crack faces. It can be compared with "reversed plasticity". Pull-out thus has the effect of stabilizing cracking situations that would be otherwise unstable, e.g. in the Tattersall and Tappin testpiece.

It may be a moot point whether pull-out should be included in the basic description of toughness, since the load bearing capacity of a cracked structure could be reduced to negligible values before the full contribution of pull-out were realized. At the same time, pull-out does improve crack stability, which is important. Also, like it or not, pull-out will usually be part of the experimentally measured toughness in typical testpieces, although the actual contribution will vary with testpiece geometry and condition of test. Of importance to experimentalists and designers in the composites field must be the realization that the effective contribution to toughness from pull-out depends

markedly on the circumstances, and each case has to be viewed separately.

Questions regarding the circumstances surrounding valid toughness testing, and associated problems of generalised yielding etc... are discussed in Appendix C.

5. Conclusions

The original proposal to NASA dated May 1971 (University of Michigan reference ORA 71-1620-KB1) aimed at producing high toughness composites without significant loss of tensile strength. This was to be achieved by special filament coating procedures. In brittle filament/brittle matrix composites as conventionally made, high strengths and high toughnesses are usually mutually exclusive.

We have been quite successful in meeting our intentions. For example, unidirectional boron/epoxy composites have been manufactured with toughnesses of over 200 kJ/m^2 whilst retaining rule of mixtures tensile strengths of some 650 MN/m^2 . The "as-received" toughness is some 50 kJ/m^2 , so that at least a 4-fold increase in toughness has been achieved. For the volume fractions employed, this represents 'fracture mechanics' stress intensity factors K of over $100 \text{ MN/m}^{3/2}$.

The new concept which has allowed us to produce these results is the 'intermittent bond', where the special coating process produces alternate regions along the filaments of high and low interfacial shear stresses, and low and high interfacial toughnesses. Then the high tensile strength characteristic of strong interfacial bonding can be combined with the high total fracture toughness of weak interfacial bonding.

Although some details of the microscopic mechanisms involved in the toughening process are ill-understood at present, a theory has been developed for composite strength and toughness which demonstrates, in broad terms, the effects of varying the coating parameters of concern. The analysis is an extension of earlier work [1]. It seems that interfacial toughness (as well as the commonly considered interfacial shear strength) is a significant property in the overall behavior. Methods are being developed to measure experimentally these elusive properties.

Scanning electron microscopy has served as a useful backup tool in our attempts to understand the mechanisms contributing to total fracture (Appendix B). For example, the question of filament/matrix relaxation after fracture in the boron/epoxy system—described by Marston [6]—and its affect on the role of the "pull-out" component of toughness has been explored. The effects of coatings on interfacial debond fractures have also been examined.

Acknowledgements

The author gratefully acknowledges the invaluable experimental assistance given by past and present students, including T.U.Marston, .Allen, and G.Streelman. Stimulating discussions were had with many teaching colleagues, among whom were R.M.Caddell, W.H.Durrant, D.K.Felbeck, .C.Ludema, and Y.W.Mai. Thanks are owed to Mrs. M.Helfen and Mrs. K.Chapin for typing various manuscripts. Throughout the tenure of the NASA Grant, r. W.B.Fichter of the Langley Research Center has been a most cooperative and patient monitor.

References

1. T.U. Marston, A.G. Atkins and D.K. Felbeck, J. Mater. Sci., 9, 447 (1974).
2. M. Piggott, J. Mater. Sci., 5, 669 (1970).
3. P.W.R. Beaumont, J. Fitz-Randolph, D.C. Phillips and A. S. Tetelman, J. Comp. Mater., 5, 542 (1971); see also J. Mater. Sci., 7, 289 (1972).
4. A. Kelly, in 'Strong Solids' (Oxford University Press, 1966).
5. J. Cook and J. E. Gordon, Proc. Roy. Soc. (Lond), A282, 508 (1964).
6. T.U. Marston, Ph.D Dissertation, University of Michigan (1973).
7. J. Mullin, J. M. Berry and A. Gatti, J. Comp. Mater., 2, 82 (1968).
8. C. Gurney and J. Hunt, Proc. Roy. Soc. (Lond), A299, 508 (1967).
9. G. T. Hahn, M. Sarrate and A. R. Rosenfield, Int. J. Fract. Mech., 7, 435 (1971).
10. Quoted by A. Kelly, Proc. Roy. Soc. (Lond), A319, 95 (1970).
11. C. Gurney and Y. W. Mai, Engr. Fract. Mech., 4, 853 (1972).
12. C. Gurney and K. M. Ngan, Proc. Roy. Soc. (Lond), A325, 207 (1971).
13. H. G. Tattersall and G. Tappin, J. Mater. Sci. 1, 296 (1966).
14. M. P. Hardy and J. A. Hudson, in 'Closed Loop', Spring 1973.

Appendix A

Derivations of Toughness Components

(i) R_{surfaces}

R_{surfaces} consists of components from filament fracture cross-sections, matrix fracture cross-sections and surfaces created by interfacial fractures. The filament cross-sectional contribution is negligible in the boron system, and we have, for random filament fracture in "untreated" composites [1],

$$R_{\text{surfaces}} = (1 - v_f) R_m + v_f \cdot \frac{l_{\text{crit}}}{d} \cdot R_{if} \quad \text{---(A1)}$$

where l_{crit} is the critical length appropriate to the (constant) τ and R_{if} is the fracture toughness of the interface between filament and matrix.

For intermittently coated filaments, we may use the fictitious l_{crit} of equation (2) in equation (A1), together with the $(R_{if})_{av}$ of equation (3) to give for mode II debonding,

$$R_{\text{surfaces}} = (1 - v_f) R_m + v_f \psi \lambda \left\{ \frac{1 - C(1 - \frac{I}{T})}{1 - C(1 - I)} \right\} (R_{ifI})_{nc} \quad \text{---(A2)}$$

Equation (A2) is given as equation (7) in the main body of text.

It should be mentioned that when the coated length is less than its own critical length, as is often the case in the experiments reported in this paper, the average debond length of coated regions is likely to be the coated length itself and not $l_{\text{crit}}/4$ which the derivation of equation (A1) strictly assumes; this introduces an error in the use of equation (A2).

(ii) R_{Cook/Gordon}

Cook and Gordon [5] suggested that if the tensile strength

of an interface ahead of a running crack were about 1/5 of the tensile strength of the matrix material, tensile debonding (mode I) would occur at the interface before the crack reached that interface. Gilliland (quoted in Kelly [10]) revised the factor to 1/50 on account of anisotropy.

Since "tensile strength" in brittle solids is a reflection of inherent flaw propagation, we may argue that

$$\frac{(\sigma_{\text{tensile interface}})_c}{(\sigma_{\text{tensile interface}})_{uc}} \approx \frac{(K_I \text{ interface})_c}{(K_I \text{ interface})_{uc}} \approx \sqrt{\frac{(R_{I\text{fI}})_c}{(R_{I\text{fI}})_{uc}}} = \sqrt{\rho_I} \quad \text{---(A3)}$$

where K_I is the stress intensity factor. For the σ ratio to be 1/5, $\rho_I \rightarrow 4 \times 10^{-2}$; for the ratio of 1/50, $\rho_I \rightarrow 4 \times 10^{-3}$.

If the filament coating procedure reduces the mode I interfacial toughness by such amounts, Cook/Gordon debonding should occur in "weak" regions ahead of a crack.

If there are N filaments in the plane of the crack, CN will be coated. If Cook/Gordon debonding occurs, the debond length will be about the coated length, in the sense that the mode I crack probably arrests in the adjacent uncoated regions where, presumably, the resistance to cracking in mode I is greater than for the coated region. Then, the debond area is some $\pi d C l_r$ (assuming complete cylindrical debonding, i.e. 'behind' filaments in the path of the advancing crack).

The work absorbed by the CN coated filaments is

$$CN \cdot \pi d \cdot C l_r (R_{I\text{fI}})_c = N \cdot \pi d^2 \cdot C^2 \cdot l_r \cdot \rho_I (R_{I\text{fI}})_{uc}$$

But

$$N = v_f \cdot \frac{4 A_{\text{nom}}}{\pi d^2}$$

where A_{nom} is the total cross-sectional area in the plane of the crack.

Whence the Cook/Gordon contribution to toughness is

$$R_{\text{Cook/Gordon}} = v_f \cdot 4c^2 \lambda \rho_I (R_{fI})_{nc} \quad \text{---(A4)}$$

Equation (A4) is called equation (8) in the main text. This contribution is appropriate only when

$$\rho_I \lesssim 4 \times 10^{-2} \text{ or } 4 \times 10^{-3}$$

For such values of ρ_I , equation (A4) gives a comparatively small contribution to toughness; Cook/Gordon debonding does, however, significantly increase the pull-out lengths, and hence the pull-out contribution to toughness.

(iii) R_{redist}

Piggott [2] and Fitz-Randolph [3] gave essentially the following expression for R_{redist}

$$R_{\text{redist}} = \frac{v_f \sigma_f^2}{3 E_f} (l_{\text{crit}}) = \frac{v_f \sigma_f^3 d}{6 E_f \tau} \quad \text{---(A5)}$$

which was the form used in reference [1] for continuously coated filaments.

For intermittently coated systems, fracture may take place in the coated or uncoated regions. Clearly R_{redist} is enhanced by the long load retransfer lengths that follow fracture in a coated region.

If we use the average interfacial shear stress given by equation (1) to represent the overall average behavior, we get from equation (A5),

$$R_{\text{redist}} = \frac{v_f \sigma_f^2 \psi \lambda d}{3 E_f [1 - c(1-T)]} \quad \text{---(A6)}$$

Equation (A6) is given as equation (9) in the text. For $C=0$, we regain equation (A5); for $T=1$, R_{redist} appropriate to

$(l_{crit})_c$ is given.

The energy dissipating mechanism is irreversible relative slip between filament and matrix in the presence of "full" interfacial bonding, with some occurring before filament fracture and some occurring upon filament "spring back" after fracture. Cook/Gordon debonding should not affect equation (A6), except in so far that the relative slip after debonding would probably be taking place in uncoated regions possessing τ_{uc} , rather than in some "mixed" coated and uncoated region possessing τ_{av} . A question is raised in the text about the magnitude of the Piggott/Fitz-Randolph term in those cases where the filament fracture strain is less than the matrix fracture strain.

(iv) $R_{pull-out}$

It was thought by Marston et al [1] that $R_{pull-out}$ was not significant in the boron-epoxy system. A toughness contribution of some 450 kJ/m^2 was given by the Cottrell/Kelly equation, which was considerably greater than the total measured toughness of $\sim 35 \text{ kJ/m}^2$. This suggested that the original interfacial shear strength was not maintained during pull-out. Moreover, electron micrography of fractured boron-epoxy specimens seemed to show that matrix material had relaxed away from the filaments after debonding.

The toughness data for the intermittently bonded composites reported in this paper consistently exceeded the contributions of "surfaces" and "stress redistribution" by significant amounts (although not by the amount that would be given by direct application of the Cottrell/Kelly expression). It must be remembered that the pull-out formula as normally quoted i.e.

$$R_{pull-out} = V_f \sigma_f^2 d / 24 \tau \quad \text{---(A7)}$$

implies complete separation of the severed parts, with the filaments pulling right out. If the crack faces in a toughness test are bridged by filaments upon completion of the measurements, (as is often the case), "full" pull-out is not achieved, and the measured toughness will fall short of predictions. In most experiments the actual pulled-out distance of relative slip between filament and matrix is less than the "average" $l_{crit}/4$ for random fracture. Rather, it is of the order of the "crack opening displacement". A modified version of the Cottrell/Kelly formula should be employed in such cases, based on the actual relative slip between filament and matrix. Although the usual formula was not appropriate, we were wrong to dismiss it completely in reference [1].

It may be shown that

$$R_{pull-out} \approx \frac{2V_f \tau' [2Dh - h^2]}{d} \quad \text{--- (A8)}$$

where D is the average distance from the end of the fracture filament to the plane of gross fracture (Fig. 14) and h is the pulled-out relative slip distance. τ' has been written in place of the interfacial shear stress τ alone, as experiments seem to indicate that a lower "frictional" interfacial traction acts after filament fracture. Putting $D=h=l_{crit}/4$ in equation (A8) will not give the usual expression as in equation (A7) because of the integration averaging method used for pull-out [4].

In intermittently coated composites, different D are appropriate for filament fractures in coated or uncoated regions, and also for those cases where Cook/Gordon debonding additionally takes place. Also, the value for the interfacial friction stress τ' has to be known. It was thought that τ' would vary with C, in the sense that if the frictional traction during pull-out was

perhaps some constant fraction of the interfacial shear stress before debonding, then τ' should decrease with C , as τ_{av} decreases with C , equation (1). However, pull-out experiments which attempted to measure τ' suggested that τ' was constant with one of the coatings, but perhaps varied with the other. Thus, two possibilities are presented in what follows:

In the absence of Cook/Gordon debonding, we may use $(l_{crit})\tau_{av}/4$ for D . Noting that for typical crack opening displacements, (a few mm), the $2h^2/d$ term may be neglected, we have from equation (A8)

$$R_{pull-out} = \frac{\nu_f \tau' \psi \lambda h}{[1 - c(1-T)]} \quad \text{---(A9)}$$

If τ' varies according to $\tau'_0[1 - c(1-T)]$, we obtain the simple result that the pull-out contribution to total toughness, measured at the same crack face opening h , is constant and equal to

$$R_{pull-out} = \nu_f \tau'_0 \psi \lambda h \quad \text{---(A10)}$$

When Cook/Gordon debonding occurs, D given by $l_{crit}/4$ is augmented by an approximate debond length $Cl_r/2$, (half the total debond length on one side of the plane of gross fracture). So, neglecting the $2h^2/d$ term,

$$R_{pull-out} = \nu_f \tau' \lambda h \left[\frac{\psi}{[1 - c(1-T)]} + 2c \right] \quad \text{---(A11)}$$

and if $\tau' = \tau'_0[1 - c(1-T)]$

$$R_{pull-out} = \nu_f \tau'_0 \lambda h \left[\psi + 2c[1 - c(1-T)] \right] \quad \text{---(A12)}$$

(v) Total Toughness

The total toughness of intermittently bonded composites is obtained by adding up the separate appropriate contributions given by the various expressions (A2, A4, A6, A9-12). For all expressions,

with $C=0$, we obtain the formula for total R for continuously coated or uncoated filaments given in reference [1], with the addition of a pull-out term. This is, of course, essentially the consequence of using the average τ given by equation (1) in the uncoated formula of Marston et al [1].

Appendix B

The accompanying scanning electron micrographs are included as supporting illustrations for some of concepts contained in the text.

Figure B1. Cross-section of triangular crack face of Tattersall and Tappin testpiece. The regularity of composite lay-up is seen. Loose "fibers" are from nylon scrim cloth.

Figure B2. Filaments bridging cracked faces in tensile specimen. The pull-out contribution from these stabilizes cracking.

Figures B3(a). Characteristic "corn-cob" surface features of boron-on-tungsten filaments.

B3(b). Impression of corn-cob surface in matrix (left hand side) before pull-out. Picture obtained from tensile specimen in which matrix layer had chipped off, thus lifting broken filaments off the matrix normally! Corn-cob features evidently persist through coating layer.

B3(c). View down pull-out 'hole'. The corn-cob impression has been smeared in the process of pull-out.

Figure B4. Pulled-out filaments in Tattersall & Tappin testpiece (PUV, C=1.0). Note oblique filament fractures (all in same direction). Loose "fibers" again from nylon scrim cloth. Some of the filaments near the apex of the specimen triangle could be pulled out with tweezers after test, indicating that such filaments had broken in bending during beam toughness test after their original fracture "inside" the beam.

Appendix C

Some Thoughts on Measuring Fracture Toughness

A series of bodies possessing cracks of increasing size will display load/extension plots in the elastic region as shown in Figure C-1, where for simplicity the bodies are considered to be linearly reversible. The type of loading may be tension, bending, etc. Those bodies with the longest cracks are the least stiff (P/u) or most compliant (u/P). If the bodies remain elastic prior to the onset of cracking, crack initiation will occur at some load on the compliance line appropriate to the 'starting crack size'. Cracking, once started, may be catastrophic or it may be slow and well-behaved. Likewise, the load during cracking may drop very suddenly, decrease slowly, remain constant or even increase, (Figure C-2). The crack behavior crucially depends on the geometry of the cracked body, and on the resistance of the material to crack propagation (i.e. on the fracture toughness).

Consider events during an increment of cracking, where at load P , the external displacement of the body changes by Δu and the crack area increases by ΔA (which in a plate-type body is $t \cdot \Delta a$, t being the uniform plate thickness and Δa the increase in crack length). The load does external work $P\Delta u$ while the elastic strain energy of the body changes by $\Delta(1/2)(Pu)$ (since the instantaneous elastic strain energy of the body is the area under the load/extension plot, i.e. $(1/2)(Pu)$). Work has to be performed in propagating the crack, and is given by $R \cdot \Delta A$ where R is the specific work dissipated in regions contiguous with the crack tip during crack spreading and is more commonly called the 'fracture

toughness'. Finally, if the crack is moving sufficiently quickly, kinetic energy of magnitude $\Delta(\text{kin})$ is generated.

Hence, equating the rates of performing internal and external work, we have for this increment of crack spreading,

$$P\Delta u = \Delta(1/2Pu) + R\Delta A + \Delta(\text{kin}) \quad (\text{C1})$$

In a quasi-static process, $\Delta(\text{kin})$ is zero. However, this does not imply that cracking is necessarily very slow: Gurney and Ngan [12] have shown that, depending on the circumstances, cracks can move up to some $\frac{c}{1000}$ before kinetic effects become significant, where c is the sonic velocity in the body. But, with $\Delta(\text{kin}) = 0$, manipulation of equation (C1) yields

$$P^2 = 2R/\frac{d}{dA}(u/P) \quad (\text{C2})$$

This is a governing equation for the so-called "compliance calibration" technique for measuring R . The rate of change of compliance with increasing crack area (i.e. $d/dA(u/P)$) may be determined graphically at various crack lengths, or if the compliances of a given specimen loaded in a prescribed way have been algebraically curve-fitted in terms of A , an analytical expression is available. Equation (c2) then gives the equilibrium loads necessary to propagate cracks of various lengths. In particular, the load at which a body starts to crack, coupled with the rate of change of compliance at the particular pre-crack starter length, will give the R value to initiate cracking. This is the way in which the equation has most often been used, and the quantity R is then called the critical strain energy release rate G_c (or γ_c) or the specific crack extension force (sic). Events during crack propagation subsequent to initiation, are usually not considered by workers who use the strain energy

release rate concept, and experiments concentrate on the load/extension diagram at "first-cracking".

There is a geometric interpretation of equation (C2) that is an extremely useful experimental tool. For a fixed fracture toughness, it follows from equation (C2) that during cracking, a plot of P versus u (i.e. the record on a typical stiff testing machine chart) will take the form of a constant R locus. Moreover, if all the irreversible work is confined to the region of the crack tip, the cracked structure will be "displacement reversible", i.e. would unload back to the origin after some cracking before the testpiece is completely broken. The ability to unload a specimen during crack propagation depends on the crack velocity which in turn depends on the specimen. In general terms, however, a testpiece with an initial crack area A_1 would load up along its compliance line (Figure C3) then crack at the load P_M given by equation (C2) using the value of $d/dA(u/P)$ at the area A_1 . Subsequently, the load/external displacement plot would follow the appropriate R locus, and if the specimen were unloaded when the crack area had increased to A_2 , the load/displacement plot would go back to the origin along the compliance line appropriate to crack area A_2 . In this way the sector area OMN represents the work done in propagating the crack from area A_1 to A_2 , i.e. $R(A_2 - A_1)$.

It is clear that depending upon the number of sectors generated during a test many estimates for R during propagation are available. The incremental sector area adjacent to the initial loading line gives the value of R for initiation (i.e. G_c). Moreover, with those fracture specimens in which the velocity changes during crack propagation, rate dependency in R may be

picked up. The P/u trace does not then follow a constant R path but cuts across the R loci, reflecting R (\dot{a}) behavior.

In experiments where displacement reversibility holds true, there is no need, of course, to unload the specimen during cracking in order to use the sector area method. If increasing crack areas (lengths) be marked upon the testing machine P/u trace, radial lines may be drawn out from the origin. Crack lengths may be monitored visually for slow crack speeds or by using conducting paint when the crack velocities are quite fast. It will be noted that the sector area technique, introduced by Gurney and Hunt [8], requires no 'compliance calibration', and thus overcomes both the difficulties of graphically measuring slopes of (u/P) vs A plots, and most particularly overcomes the problems caused by rate dependent moduli upon compliance calibration measurements.

Many workers tackle fracture problems by modifying the classical Griffith equation for cracking. In the present nomenclature we have

$$\sigma = \sqrt{\frac{ER}{\pi l}} \quad (C3)$$

where σ is the stress on the boundary of a large plate of Young's modulus E that causes extension of a small crack of length $2l$. The Griffith case is a particular solution of equation (C2) where $d/dA(u/P)$ for a small crack in a large plate is obtained from Inglis's mathematics, see Gurney and Hunt [8]. In Griffith's original presentation, the work of fracture was identified with the surface free energy (γ_s) of the fractured glass specimens, and since surface chemists define γ_s with reference to each side of the crack, equation (C3) is more usually written as

$$\sigma = \sqrt{\frac{E \cdot 2\gamma_s}{\pi l}} \approx \sqrt{\frac{E \gamma_s}{l}} \quad (C4)$$

since then, $R = 2\gamma_s$.

Equations (C3) and (C4) may be used to measure γ_s by noting the stress at which fracture ensues in a specimen containing a precrack of length $2l$.

Another approach which measures a quantity often called γ , (and which also is referenced to both sides of the crack), takes the total area under a load/extension plot as the work dissipated in fracture and divides by twice the generated crack area to obtain the so-called 'work of fracture' [e.g. Tattersall and Tappin, reference 13]. Essentially the whole P/u diagram is considered as one big sector area. Care must be taken, however, to account for residual strain energy if the specimen is not cracked through, and if the load is still finite, when the measurements are taken. That is, in Figure C4, the recoverable elastic energy OQS must be subtracted from OMQS. Sometimes this is not done, leading to overestimates for γ . The technique clearly "averages" the specific work of fracture, and does not pick up variations during propagation, unlike the sector area method.

Finally we come to the "stress intensity factor" (K) of fracture mechanics as a measure of toughness. This quantity comes about from considerations of the detailed elastic stress fields around a crack tip; cracking initiates when K reaches a critical value K_c . Physically, K is an alternative means of expressing the fact that cracking ensues when the strain energy release rate from the cracked structure (G) reaches the critical value (G_c) that will feed the crack at the rate required for propagation.

K and G or R are related by $G \text{ or } R = K^2/E$. All Formulae for K are essentially the same as equation (C2), where the $d/dA(u/P)$ term has been worked out in the K mathematics. K_c is most often used like G_c for crack initiation only — without regard to subsequent events — although it is presumably in order to think of a K during propagation given by \sqrt{ER} . With rate dependent materials, the appropriate value for E, based upon crack tip strain rates, is debatable.

People use the word "stability" to mean different things in the field of cracking. In the fracture mechanics literature, an unstable crack is one that continuously propagates after any "sub-critical" growth that may occur before the maximum load or "pop-in" load from which K_c or G_c is calculated. Subsequent cracking is often called 'fast' even though in real terms it is not fast, and indeed may readily be arrested. It seems more sensible to define an unstable crack as one that is quickly accelerating with every-increasing velocity. Whether a given crack in a given shaped testpiece will be unstable or stable depends upon the imposed testing constraints. The solution of equation (C2) for the particular crack size in the particular testpiece shape determines whether the crack will behave stably or unstably. Gurney and Mai [11] give a thorough coverage of crack stability and show that it depends upon the geometric properties of the crack/testpiece combination ('geometric stability factor', or 'gsf') ^{and upon any rate-} dependent toughness behavior. Clearly, materials whose R increases with crack velocity (i.e. $dR/d\dot{a}$ is positive) tend to produce stable cracks because they provide a sink for the energy released from the testpiece. Even so, stable cracking is possible with $dR/d\dot{a}$ negative

materials if the gsf is big enough.

Care must be taken not to confuse fast fractures with unstable fractures. As already mentioned, Gurney and Ngan [12] have shown that little error in R occurs if $\Delta(kin)$ is ignored in equation (C1) up to quite high velocities. In typical laboratory-size testpieces, the crack can propagate through the specimen in a very short time at velocities which are small compared with $c/1000$.

It is difficult at first sight to distinguish between fast 'stable' fractures and actual unstable fractures. The latter occur in hard machines when the increment of u that satisfies equation (C1) is negative, i.e. when there is so much strain energy present in the system at crack initiation that the test-piece can afford to unload, giving back work ^(MNVW) to the loading device, yet still have enough strain energy to feed the crack at the appropriate rate. The R locus points back to the origin (Figure C5). Since testing machine screws do not normally reverse in a test, the situation is unstable and the testpiece goes "bang" with an instantaneous vertical drop in load.* The triangular area on the load diagram ^(OMW) is thus an upper bound for R . Use of K or G formulae in unstable situations is permissible, however, because the expression takes the instability into account. Indeed the Griffith case is inherently unstable, unless $dR/d\dot{a}$ is excessively positive.

In the case of toughness testing of composites, it is a

* A report by Hardy and Hudson [14] demonstrates how suitable control circuitry for crosshead displacement permits "unstable" R loci to be followed.

common occurrence to find filaments bridging the fracture surfaces after the crack front has passed by. As those filaments pull-out during subsequent crack propagation, irreversible work is done, and upon unloading the testpiece is not "displacement-reversible", further irreversible work being performed. Often the cracked testpiece remains yawed open after testing. Filaments bridging the crack faces stabilize cracking situations that would otherwise be unstable. Figure C-5 and Figure 13 demonstrate this very well in connection with the Tattersall and Tappin testpiece.

One further consideration in toughness testing that is most important, but often times is overlooked, relates to specimens that do not close up after cracking. The foregoing paragraph mentioned this possibility with the geometric interference of fibers bridging the crack faces preventing crack closure. In the absence of bridging filaments, residual crack openings occur for two distinct reasons. The first relates to yielding in the testpiece at regions remote from the crack tip, as shown in Figure C-6. Clearly it is difficult, from the P/u diagram to differentiate between the cracking work performed at regions contiguous with the crack tip and the generalised yielding performed away from the crack tip. It is seen that, for a given material, the occurrence of generalised yielding depends crucially on the geometry of the specimen; for example, if the "arms" of the edge crack testpiece in Figure C-6 were bigger, yielding may be prevented. Generalised yielding is more likely the larger the toughness/strength ratio (i.e. the larger the K/σ_y ratio). Hence, generalised yielding is a bane in the toughness testing of low strength/high toughness materials, and is a problem which is additional to difficulties of ensuring 'plane strain' fractures.

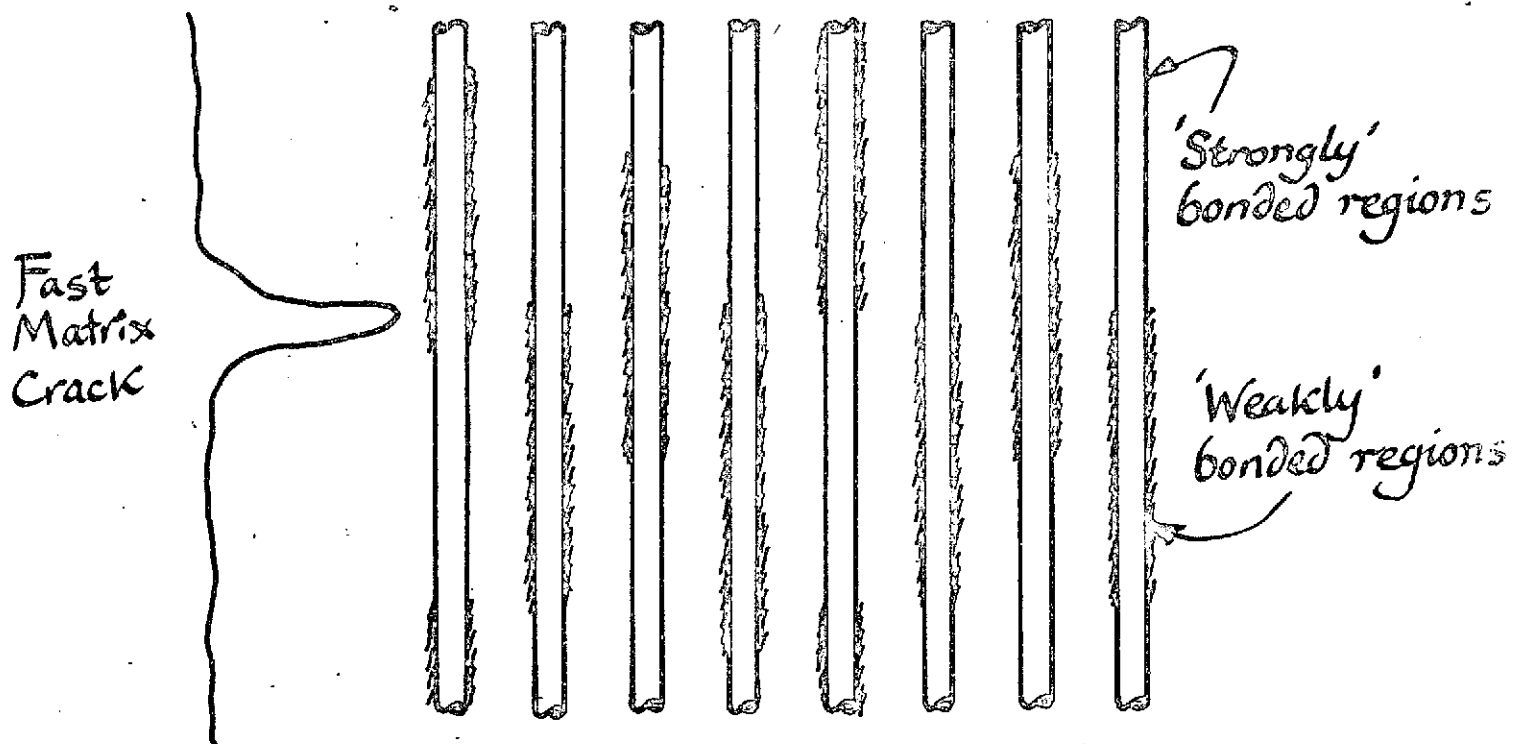
-4/-

The second reason that cracks can remain yawed open concerns large crack tip plastic zones, such as seen in the tough polymer polycarbonate. The zone necks down during formation, so that the specimen is effectively restrained by a residual moment at the crack tip, giving a residual crack opening of OT on unloading, Figure C-7. The foregoing can occur without generalised yielding. If, therefore, it be argued that all the irreversible work must be crack-ing work, (there being no generalised yielding), and that the residual crack opening is caused merely by a geometric interference effect, (it also being presumed that there has been no reversed plasticity in the crack tip zone upon unloading), there is a means of "rescuing" valid toughness data from such diagrams as Figure C-7, as follows: The loading/unloading sequence would be OMNT. If however at N, the specimen be saw cut along the crack path beyond the crack tip zone into virgin material, the load will drop to Q, and if all the foregoing postulates are valid, the specimen should unload to the origin, O. Then it is presumably valid to generate sector areas such as ONS from which valid R data may be obtained. There are uncertainties about possible differences between the work to grow the large zone to its critical (imitation) size at the crack tip in the first instance, and the subsequent incremental work during propagation, but such things can be resolved by experiment. The main thing is that diagrams such as OMNT in Figure C-7 may give valid data, whereas apparently similar diagrams such as OMNST in Figure C-6 will not do so. Interesting questions may be posed regarding J -integral circuits, and the answers obtained, in situations such as Figures C-6 and C-7.

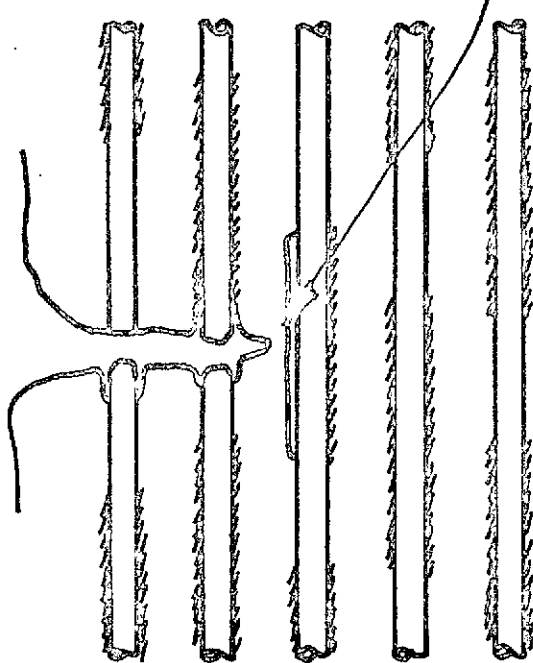
Captions for Figures

1. The Intermittent Bond and Cook/Gordon Debonding.
 2. Intermittent Bond Geometry.
 3. Critical Shear Transfer Lengths.
 4. Photograph of Coating and Tape Making Apparatus.
 5. Edge-Crack Fracture Toughness Specimen.
 6. Gurney's Sector Area Method for R.
 7. Testpiece Buckling at Backface.
 8. Tensile Results for Intermittently Bonded Composites.
 9. Toughness Results for Intermittently Bonded Composites.
 10. Warped Testpiece Owing to Generalised Yielding of Arms in High Volume Fraction, High Toughness Specimen.
 11. Photograph of Pull-out Lengths, 38 mm long.
 12. Photograph of Crack Opening in C=0 and C=1 Specimens.
 13. Differences in Unstable and Stabilized Tattersall and Tappin Testpiece Toughness Loci.
 14. Geometry of Pull-out Lengths in Presence of Intermittent Bonding.
-
- B1. Filament lay-up in Tattersall & Tappin testpiece.
 - B2. Filaments bridging crack faces.
 - B3(a). Corn-cob topography of boron filaments.
 - B3(b). Corn-cob impression in matrix.
 - B3(c). Smeared corn-cob feature after pull-out
 - B4. Pulled-out filaments in high percentage coat Tattersall & Tappin testpiece.
 - C1. Cracked body compliances with different crack lengths (areas).
 - C2. Possible R-loci
 - C3. Gurney's sector area method for R (displacement reversible situation).

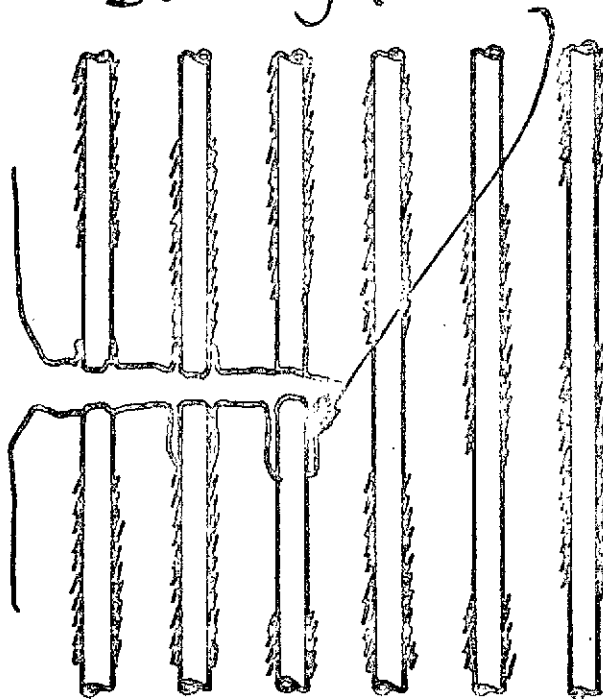
- C4. Meaning of term 'work of fracture' (γ)
- C5. Energy changes in unstable cracking situation.
- C6. Displacement-irreversible situation caused by generalised yielding at regions remote from crack.
- C7. Displacement-irreversible situation caused by large crack-tip plastic zone (no generalised yielding).



Cook/Gordon Debonding (Mode I)



Outwater/Murphy Debonding (Mode II)



NOT REPRODUCIBLE

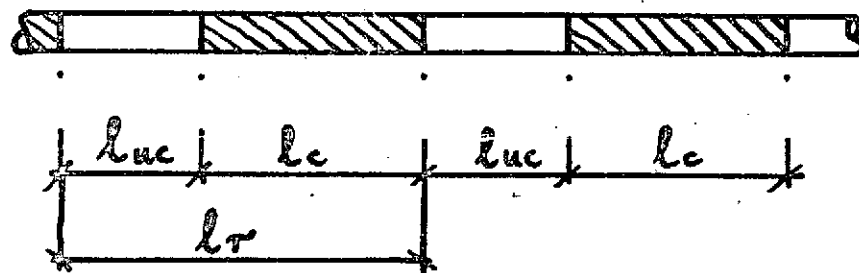


Fig. 2

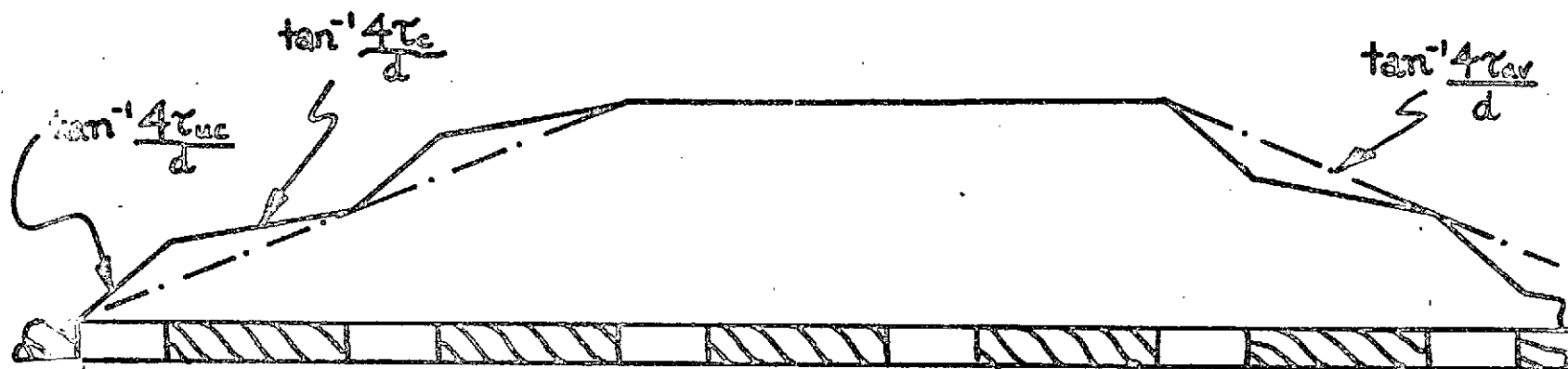


Fig. 3

46<

NOT REPRODUCIBLE

47<

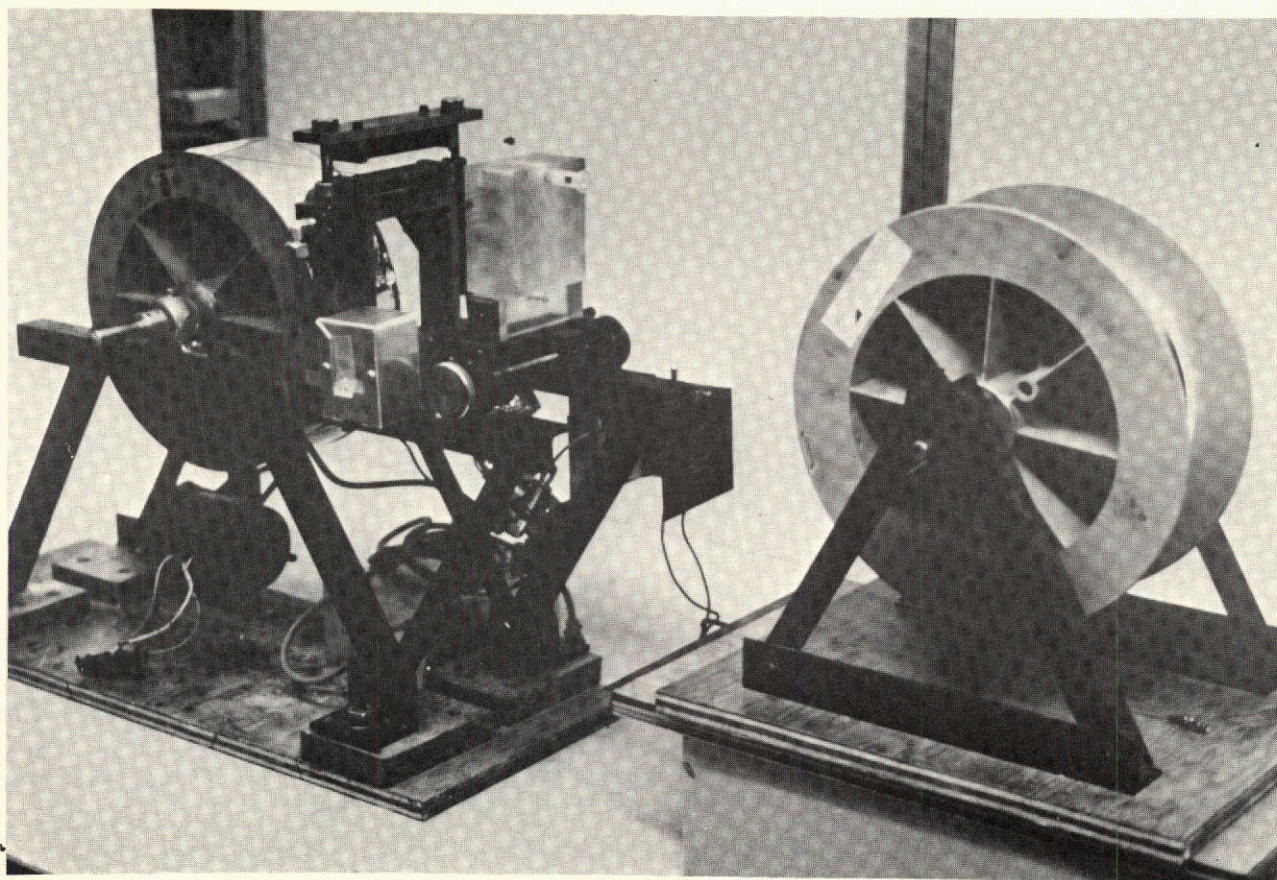


FIGURE 4

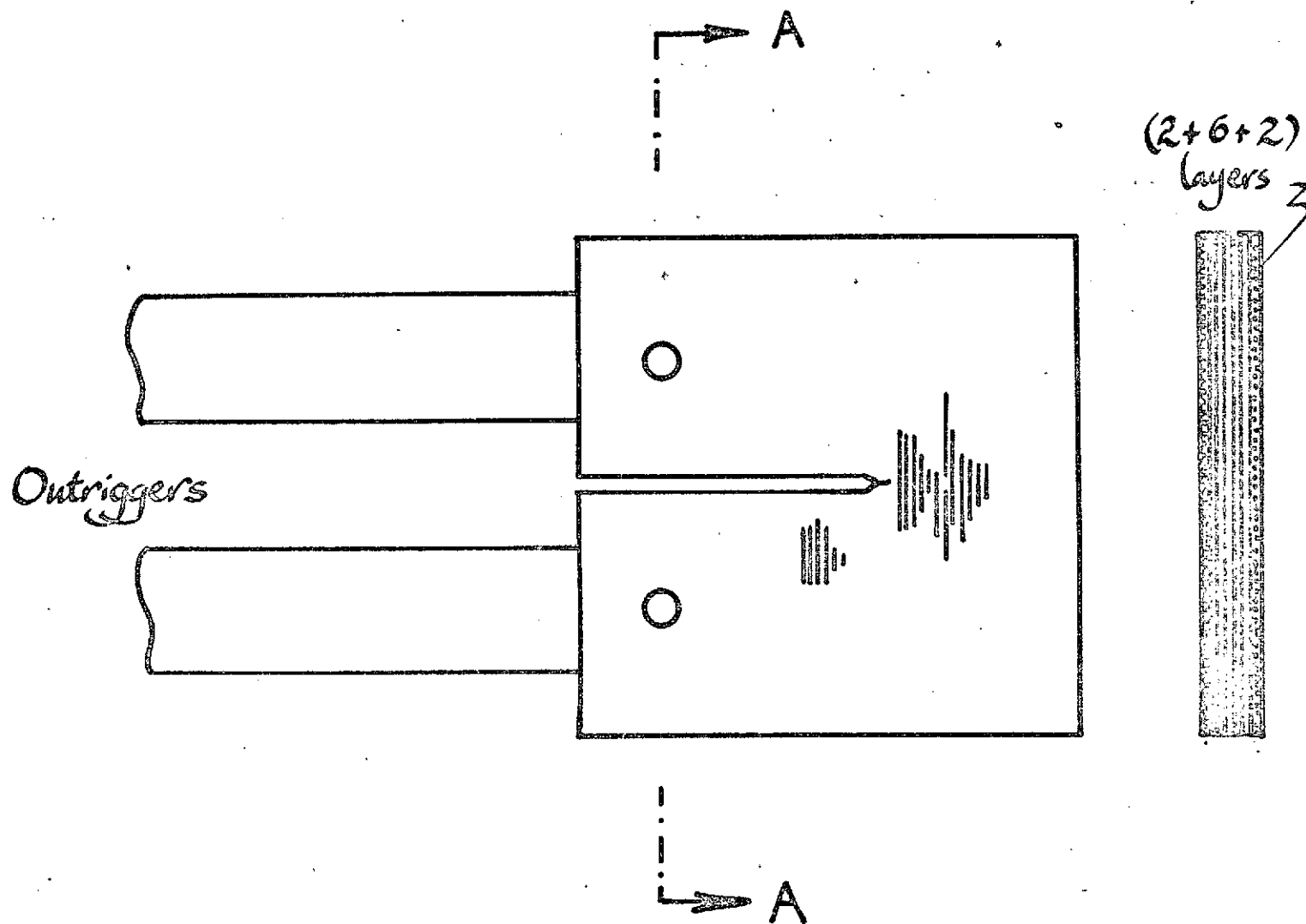
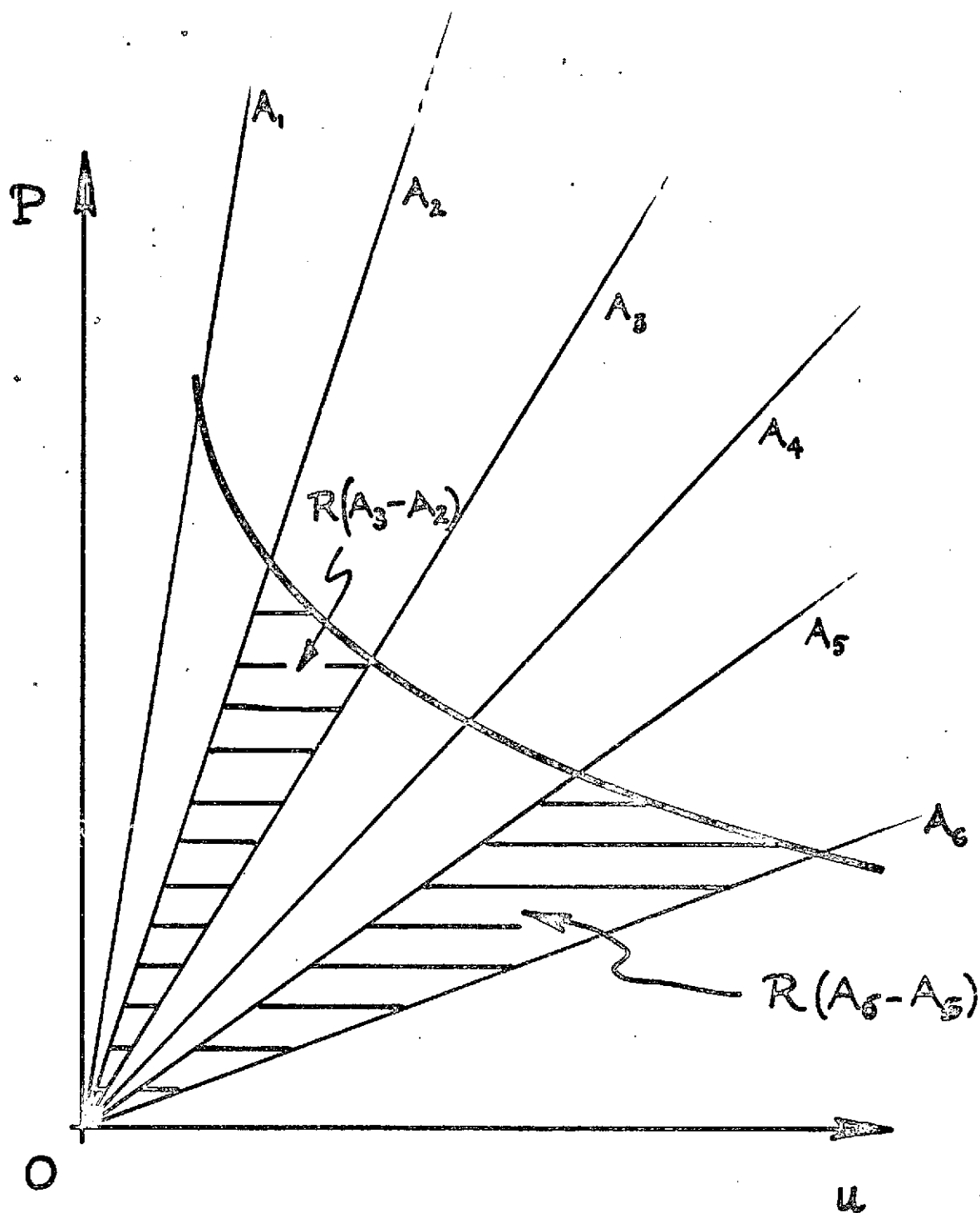


Fig. 5



NOT REPRODUCIBLE

Fig. 6

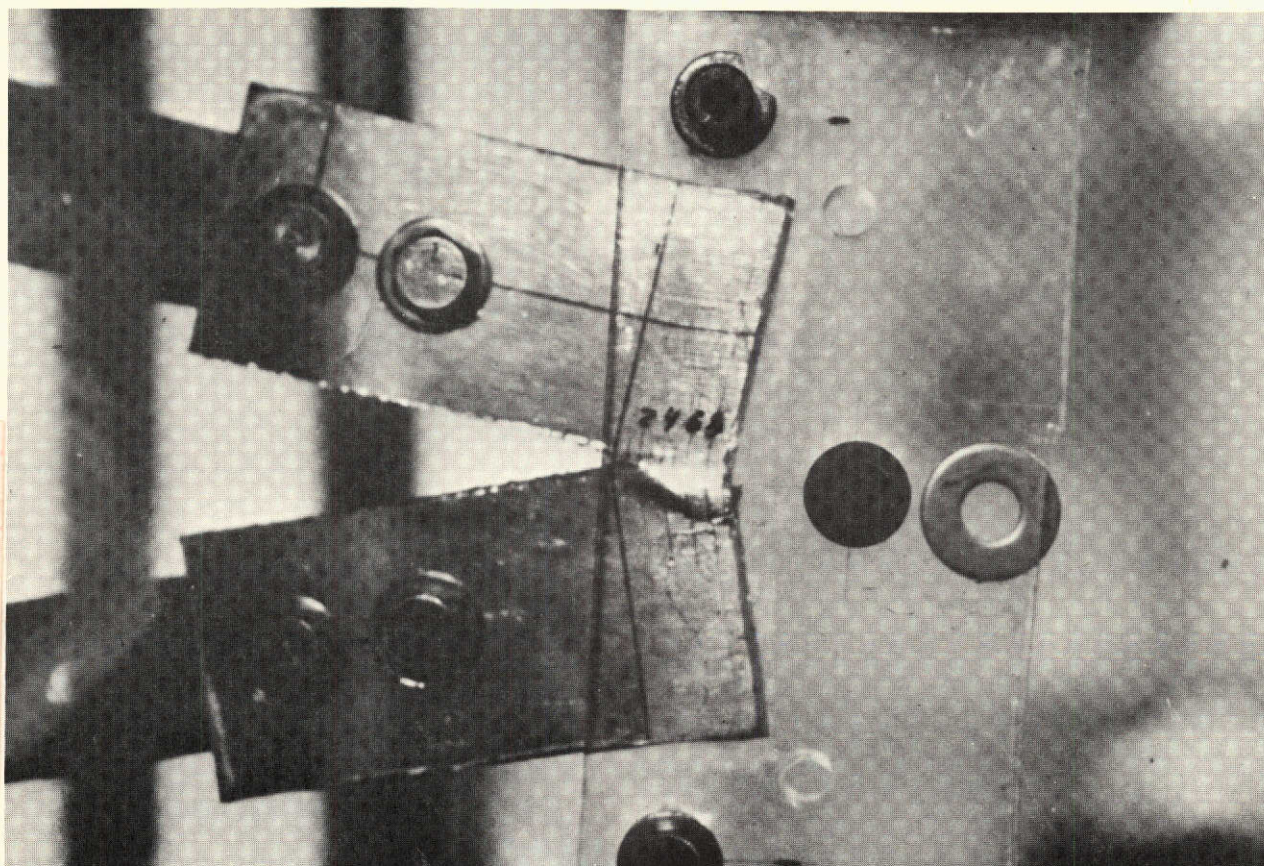


FIGURE 7

NOT REPRODUCIBLE

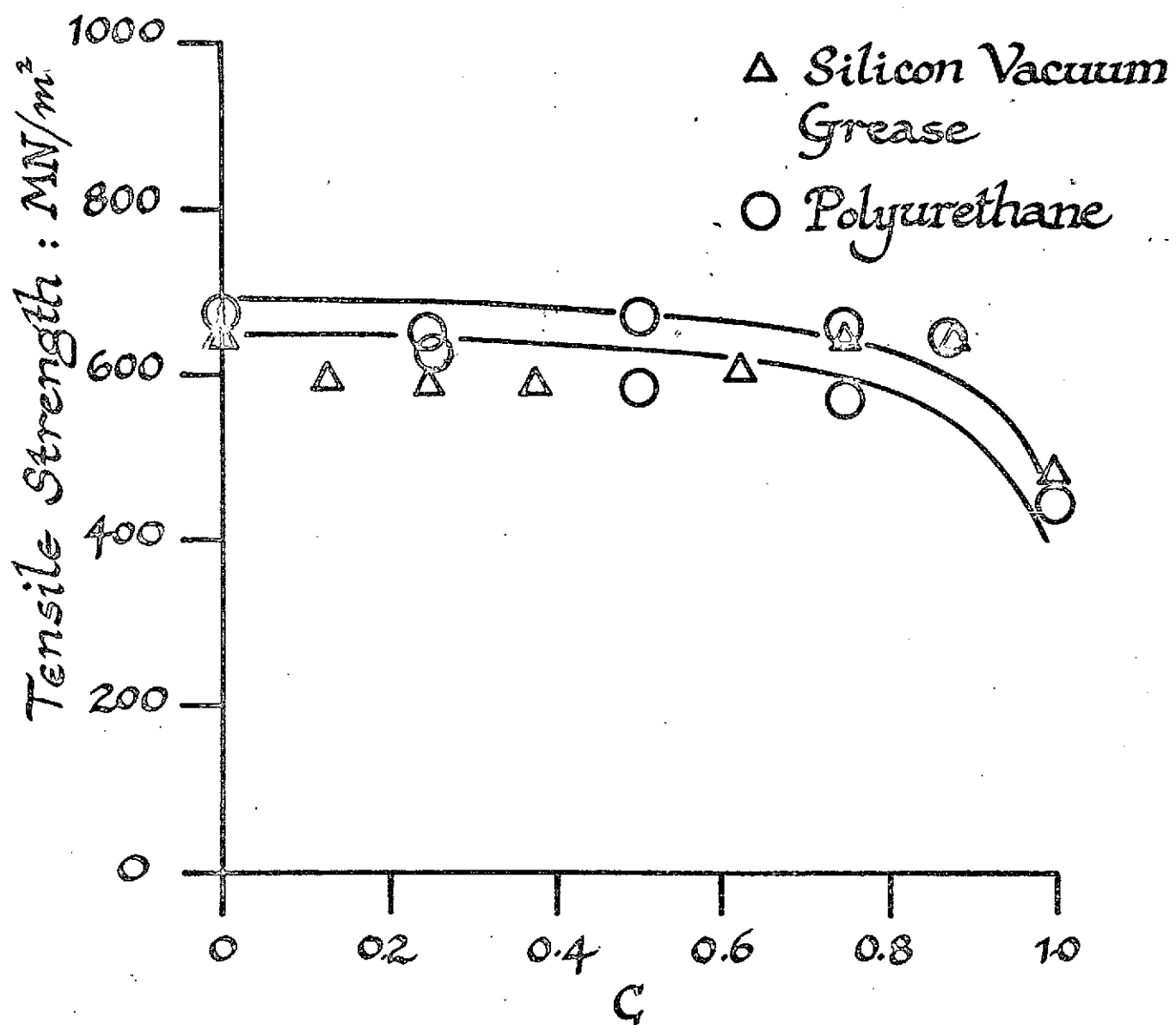
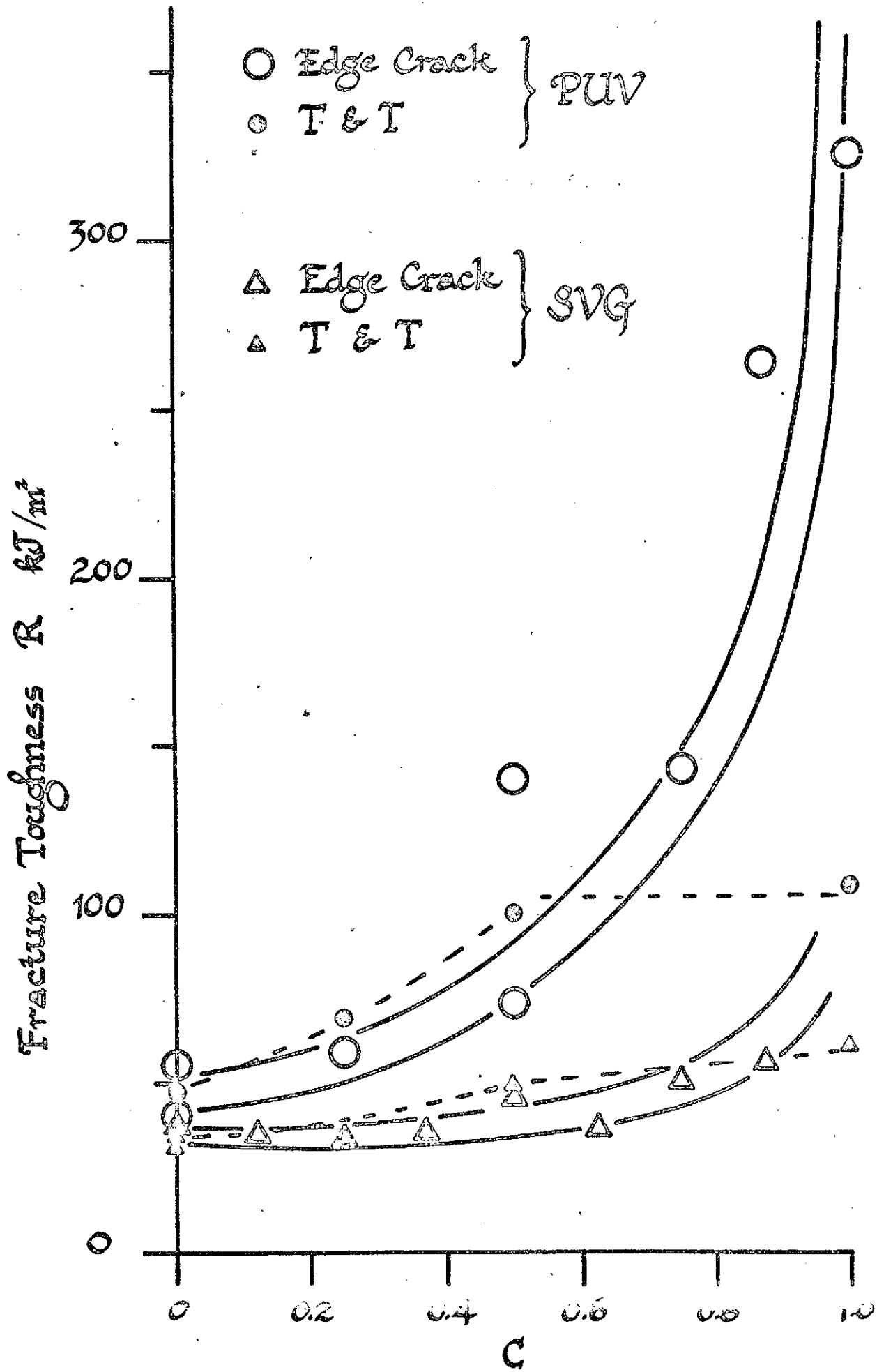


Fig. 8



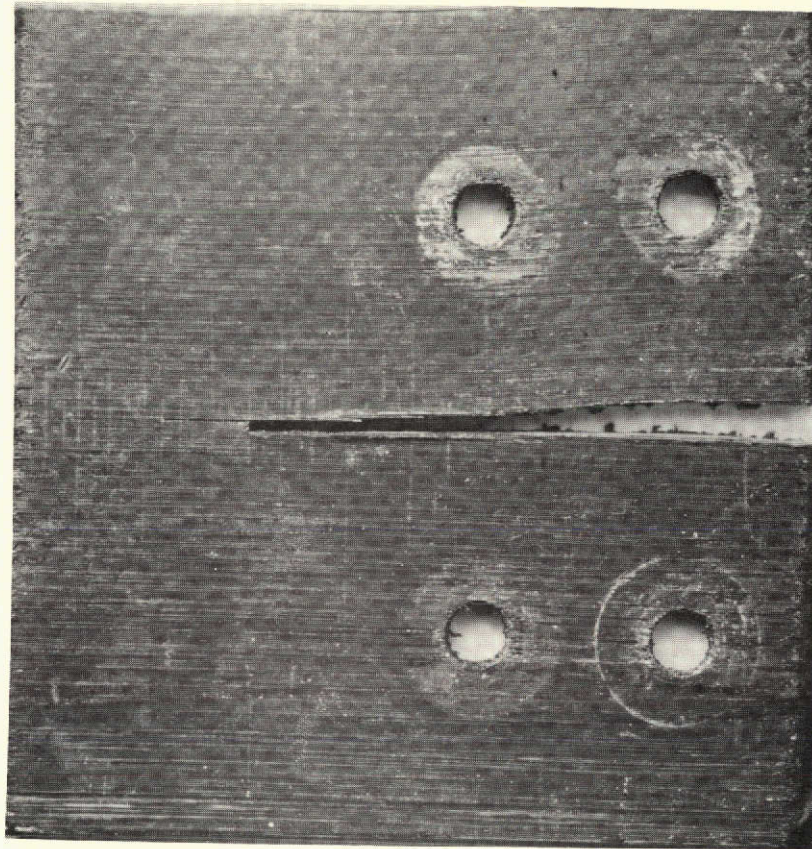


FIGURE 10

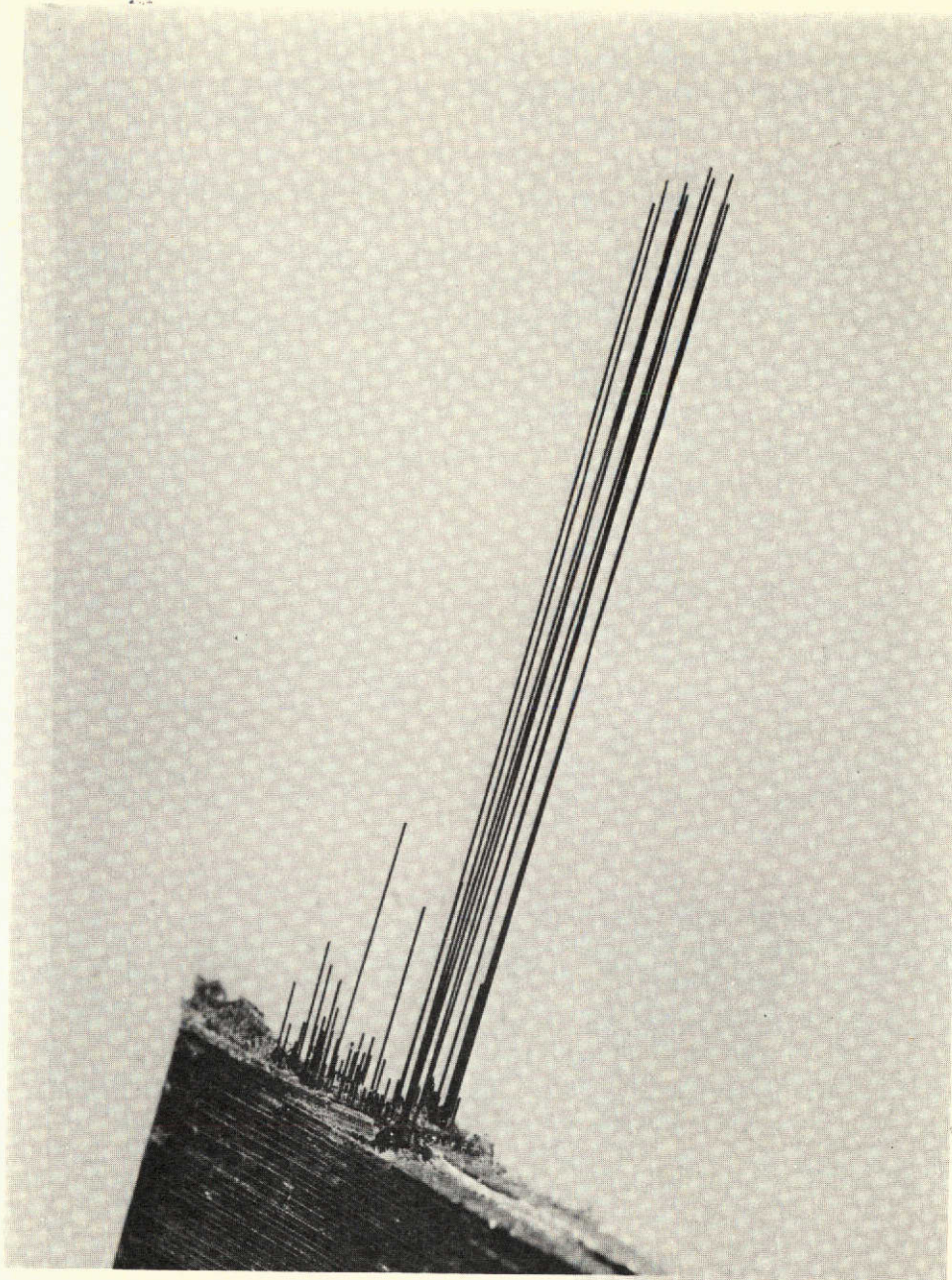


FIGURE 11

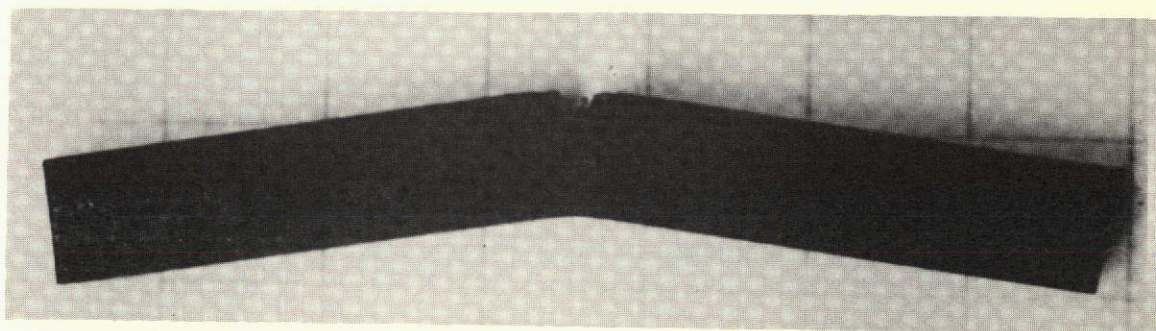
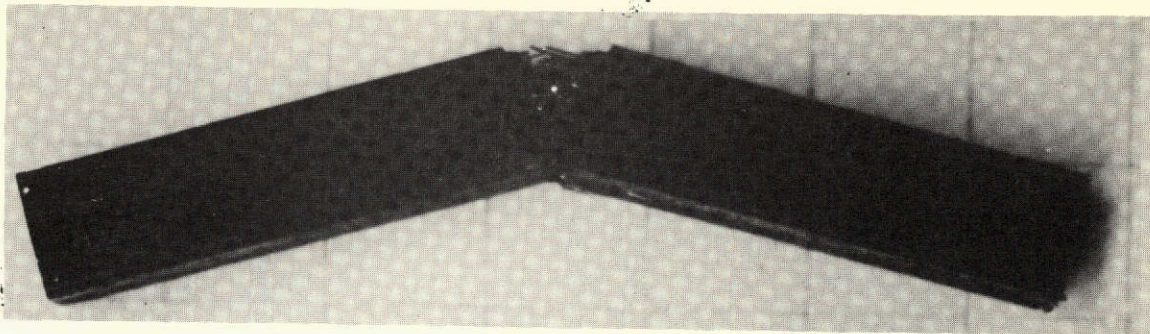


FIGURE 12

...roduced at the

P : Newtons

NOT REPRODUCIBLE

1000

500

0

0

1

2

3

x : mm

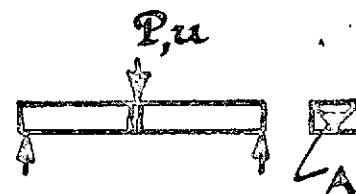
 $R = 100 \text{ kJ/m}^2$ $A = 0 \text{ mm}^2$ $A = 2 \text{ mm}^2$ $A = 4 \text{ mm}^2$ $A = 6 \text{ mm}^2$ $A = 8 \text{ mm}^2$ $R = 10 \text{ kJ/m}^2$ 

Fig. 13

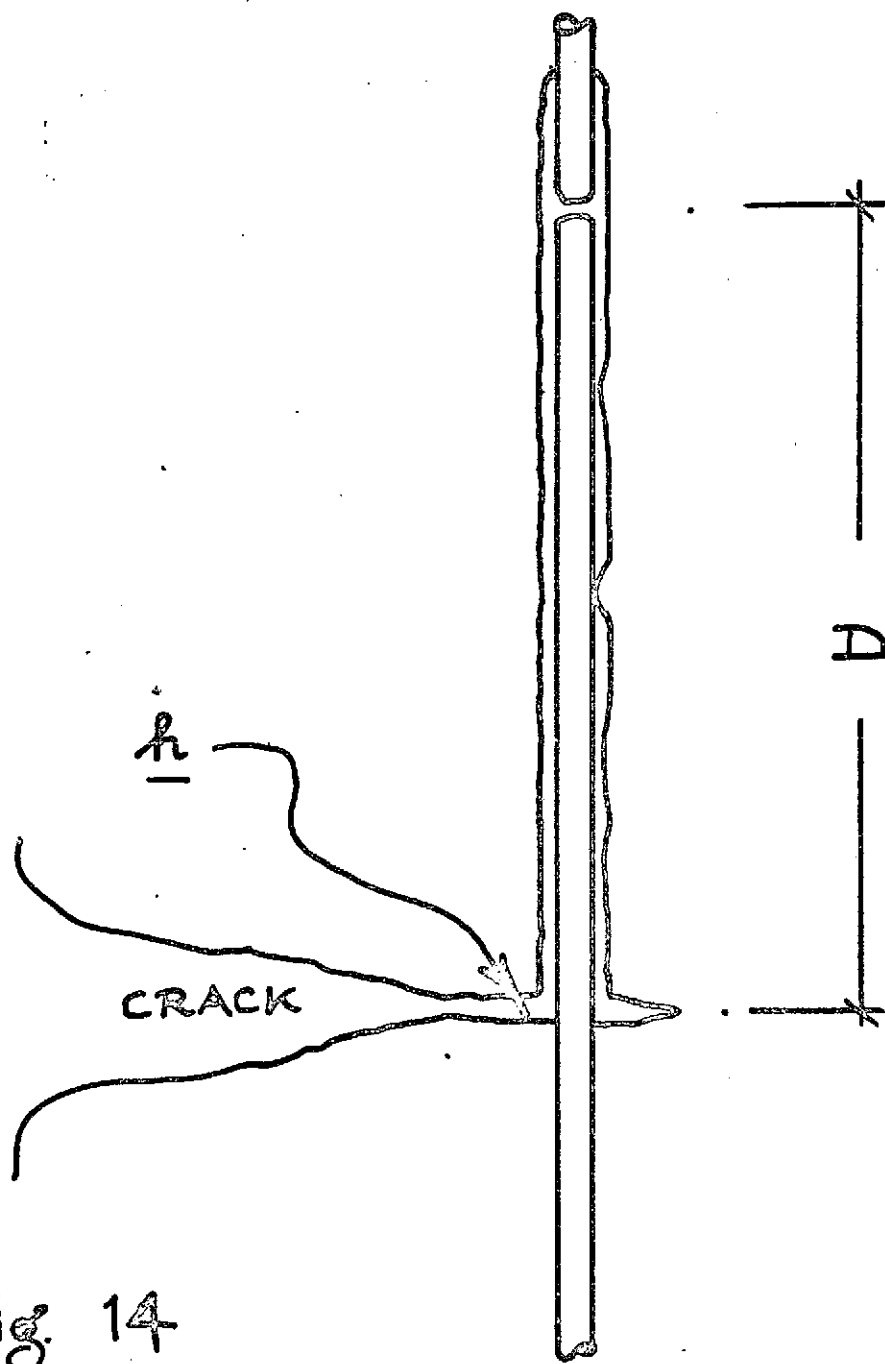


Fig. 14

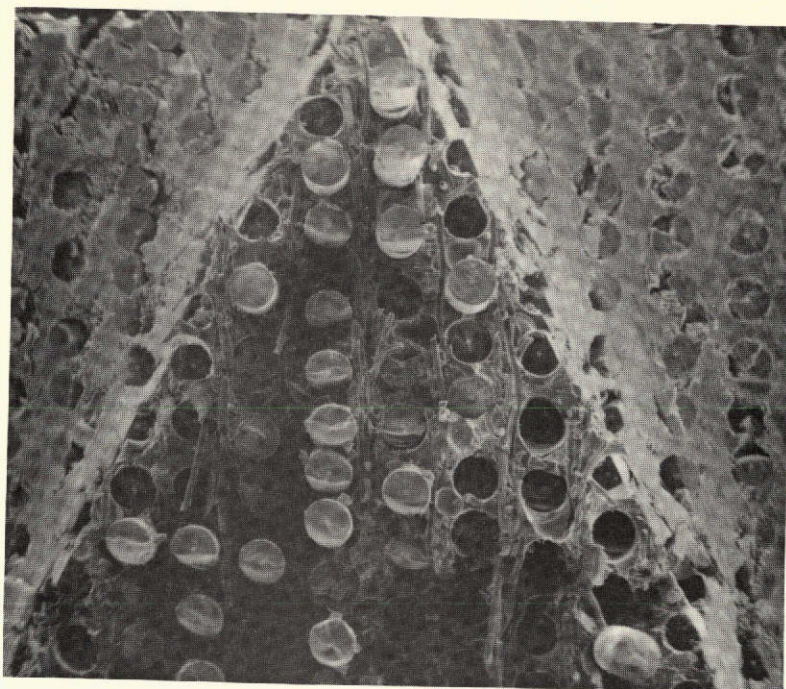


FIGURE B-1

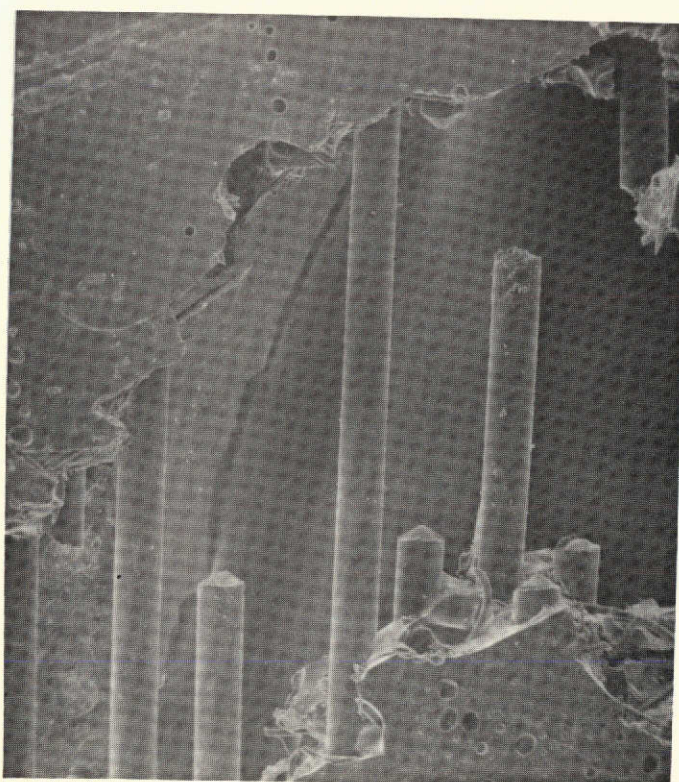


FIGURE B-2

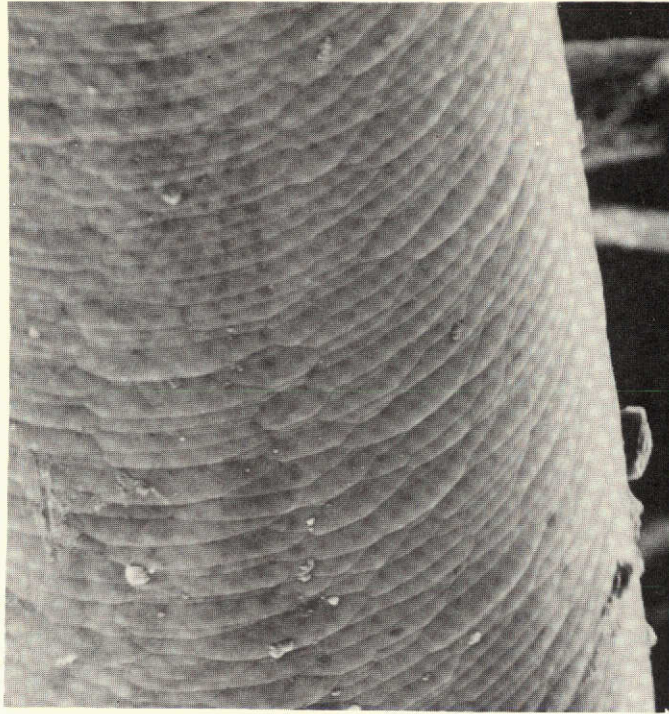


FIGURE B-3(a)

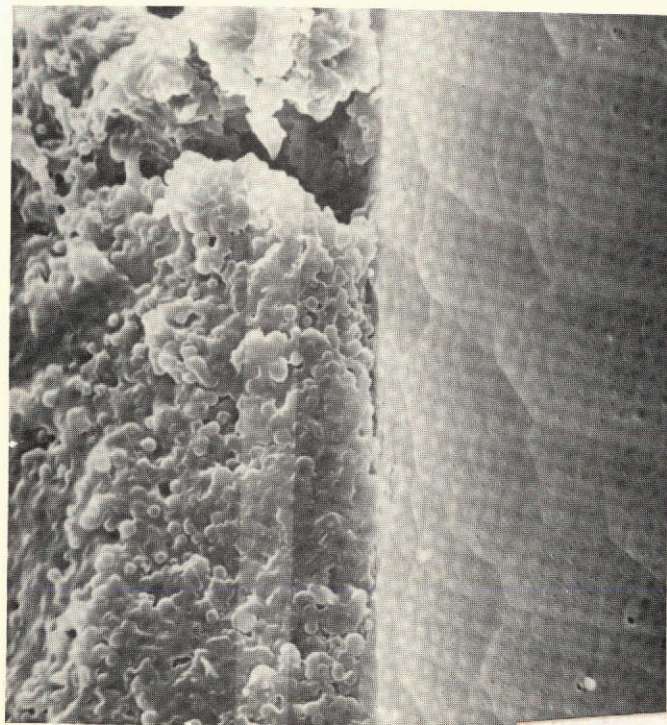
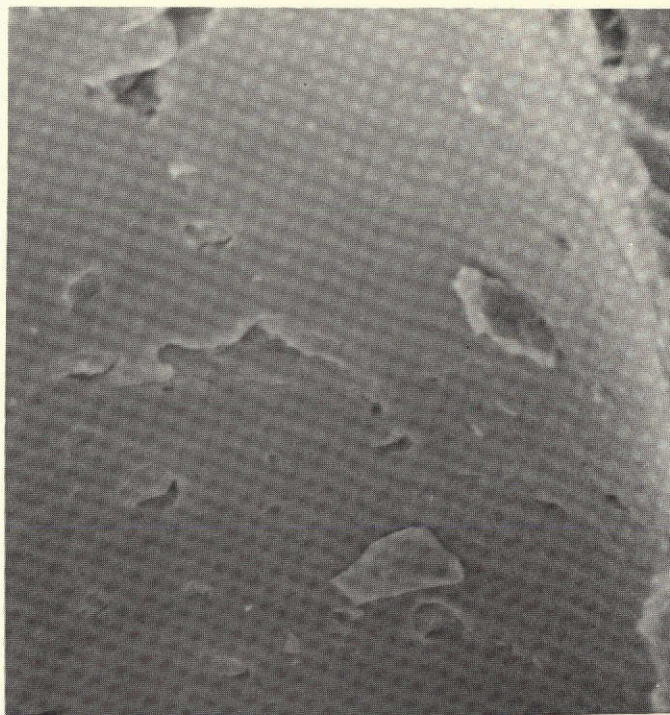


FIGURE B-3(b)



This page is reproduced at the

FIGURE B-3(c)

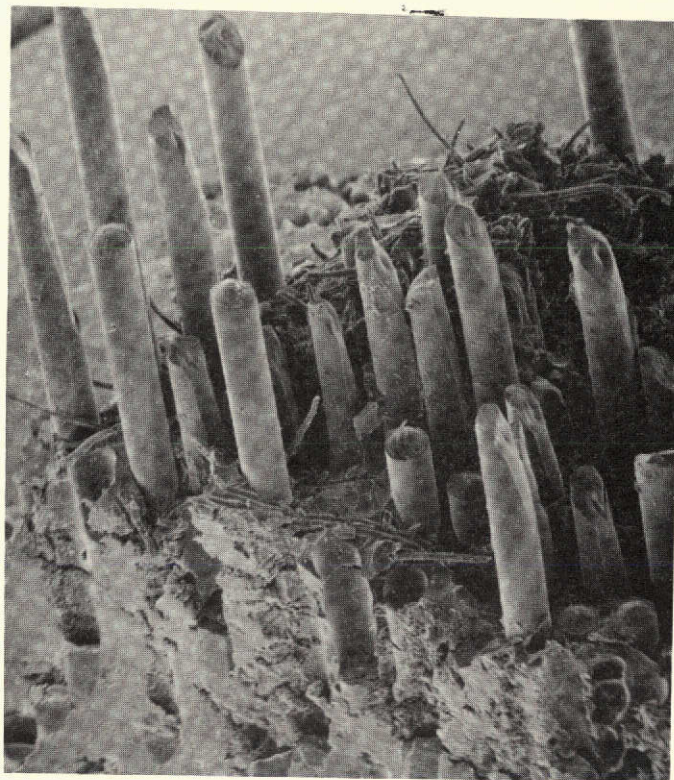


FIGURE B-4

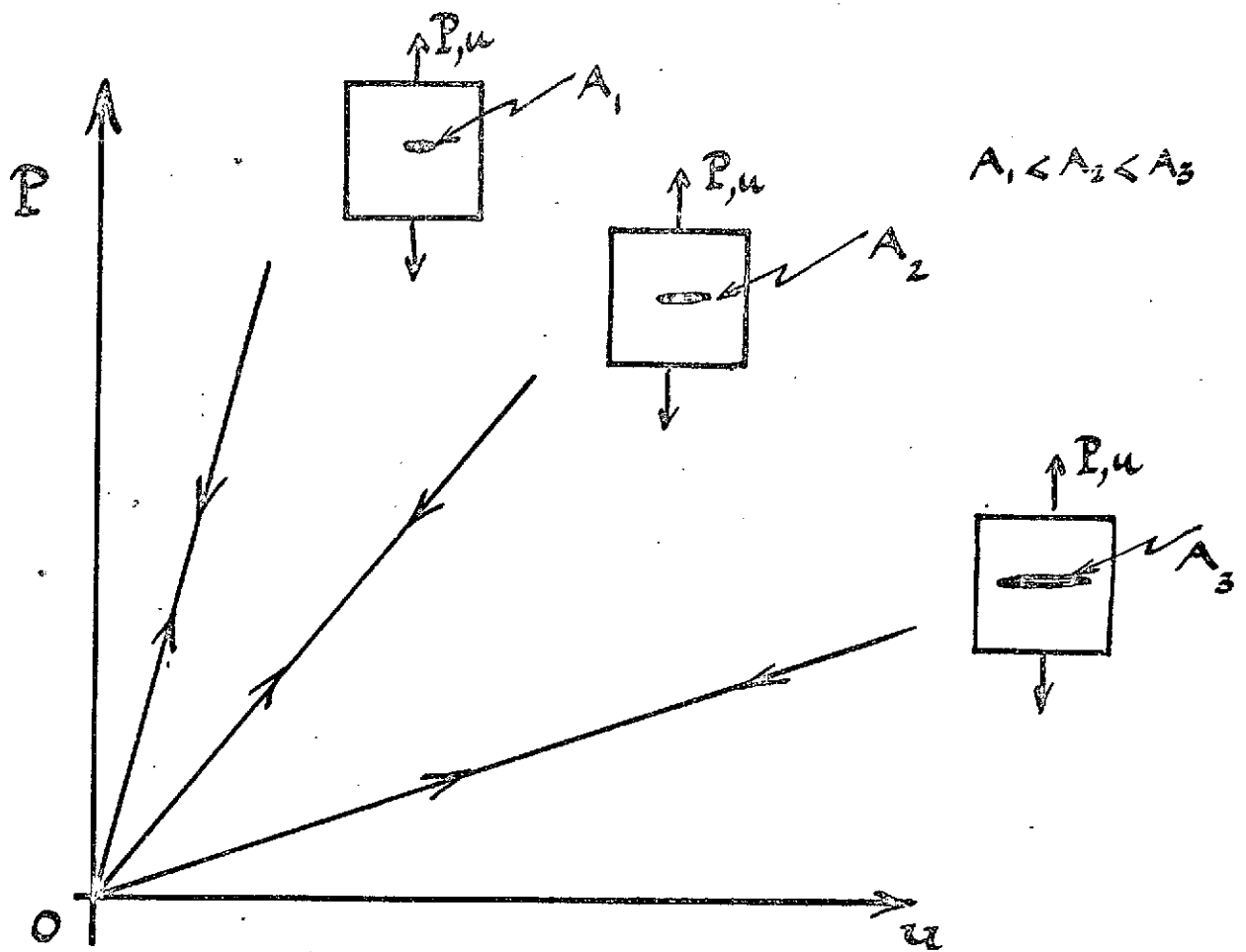


Fig C-1

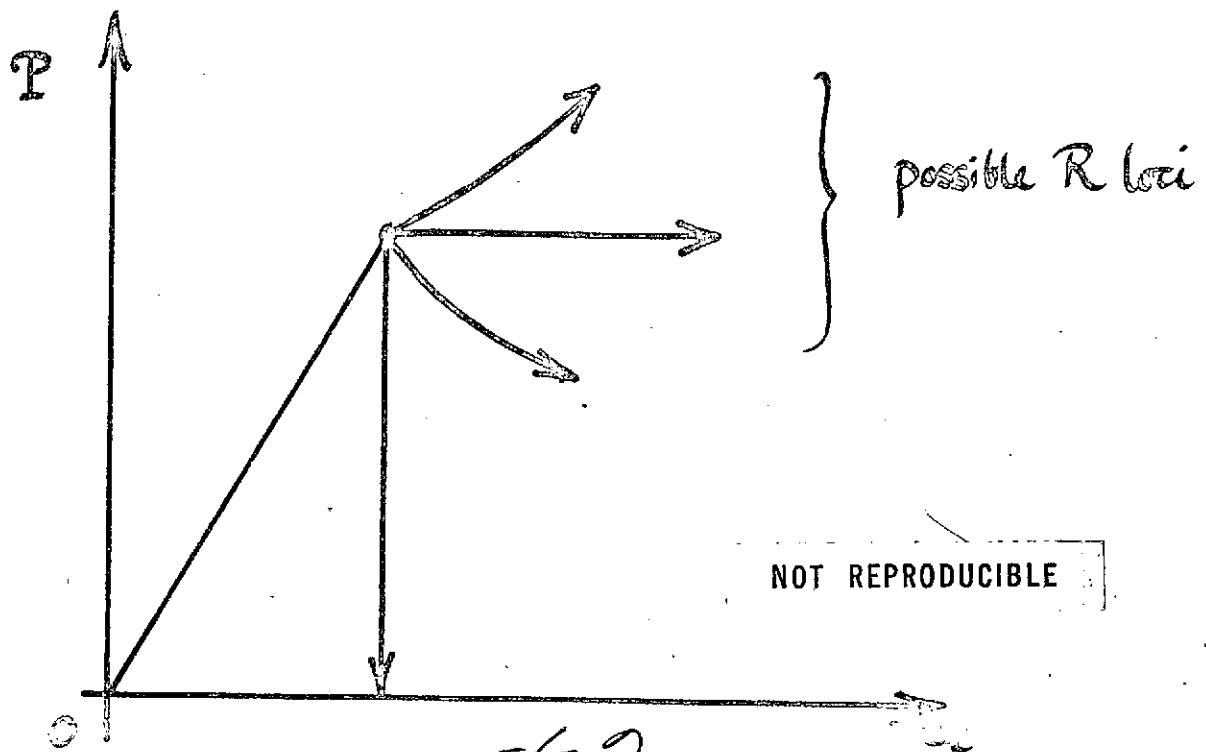


Fig C-2

